THE UNIVERSITY OF MANITOBA

A SYSTEM

FOR PERMITTIVITY MEASUREMENT

IN THE TIME DOMAIN

by

MAREK T. FABER

A THESIS

SUBMITTED TO THE FACULTY OF GRADUATE STUDIES

IN PARTIAL FULFILMENT OF THE REQUIREMENTS FOR THE DEGREE

OF MASTER OF SCIENCE

AGRICULTURAL ENGINEERING DEPARTMENT

WINNIPEG, MANITOBA

May 1975

"A SYSTEM
FOR PERMITTIVITY MEASUREMENT
IN THE TIME DOMAIN"

by

MAREK T. FABER

A dissertation submitted to the Faculty of Graduate Studies of the University of Manitoba in partial fulfillment of the requirements of the degree of

MASTER OF SCIENCE

ABSTRACT

Fast measurements are especially important in investigations of the dielectric properties of biological substances (where test materials have to be measured in many different conditions). An experimental system for fast permittivity measurements over a wide frequency range has been developed. The lumped capacitance method, which requires a very small sample, is employed.

The measurements are performed in the time domain and the data transformed into the frequency domain by means of a digital computer. The speed and simplicity of measurements have been achieved by automatic analog to digital conversion of the time domain curves. Software for processing of the experimental data has been developed.

ACKNOWLEDGEMENTS

I wish to express my grateful appreciation to Dr. S.S. Stuchly for suggesting this thesis subject and for his supervision and encouragement throughout the entire work.

Special thanks are due Dr. M.A.K. Hamid and Professor A. Jakobschuk for their interest and valuable comments.

I would like to express my deep graterulness to Dr. G.E. Laliberte for his assistance.

I also wish to acknowledge my sincere thanks to Mr. A. Hamid and Mr. W.S. Matulewicz, my colleagues, for their interest and profitable discussions.

I am pleased to express my grateful thanks to my wife Anna who has taken on the hardships imposed by an ever absent husband. I am indebted to her for her patience and encouragements.

TABLE OF CONTENTS

LIST OF FIGURES AND TABLES

CHAPTER 1

INTRODUCTION

Knowledge about the electrical properties of agricultural materials becomes increasingly significant as agricultural technology becomes more sophisticated, as new uses for electric energy are developed, and as new methods, processes and devices come into being which utilize or are influenced by the electrical nature of materials. The electrical properties of animal tissue have been intensively investigated since the end of the last century /1/. The principal reason for these investigations has been the interest in effects of electric currents and electromagnetic fields on human beings, the interest in understanding the conduction of electrical signals in animal tissue, and in using electrical methods for the study of the structure and function of biological systems.

Electrical properties of food products have generally been of interest for two reasons. One relates to the possibility of using the dielectric properties as means for determining quality factors. The other has to do with the absorption of energy in high-frequency dielectric heating or microwave heating applications employed in the processing of food materials.

There has been much interest in dielectric properties of grain and seeds for many years because of many potential applications, including the use of electric energy for mois-

ture measurements, grain drying, stored grain insect control and remote sensing for measurement or process control.

Electrical properties of agricultural and biological materials vary widely and are dependent upon many factors. The basic and most important factors are: frequency, temperature, moisture content, density, pressure and anisotropic nature in the structure of the material.

Precise values for any particular substance under a particular set of conditions can only be obtained by careful measurements. There is only one way to examine the dielectric properties of materials - to tests the substance by varying one factor while all others are held constant. But there is an infinite number of sets of conditions for which the material may be tested. Thus, an enormous number of measurements must be performed and therfore the speed of the employed method is extremely important.

A large number of methods has been developed and many different techniques have been used to investigate the dielectric properties of materials. The classical methods are based on measurments of electrical quantities at one fixed frequency. Then the frequency is changed and the measurements are repeated. The dielectric properties of test material are not determined directly. The steady-state approach in the frequency domain requires many laborious techniques but

nowadays these techniques are becoming faster since high-speed computers are used in the processing of experimental data /2/. Furthermore, frequency domain methods can be speeded up by use of a sweep generator and sutomation of measurements.

An alternative approach based on measurements in the time domain offers many advantages. Instead of sweeping the frequency, a pulse is generated which has a frequency spectrum spread over a wide frequency range /e.g., a fast rise time step function/. Such a pulse is then applied to the test sample and a response of the substance to this excitation is observed. The dielectric properties of the material can be obtained by calculating the Fourier Transforms of excitation and response signals. These time-to-frequency domain conversions have to be done by a digital computer. It is possible to decrease or even eliminate human participation in this whole link, and, thus, make the measurement very fast.

It is the object of this research to develop a system for fast measurement of the dielectric properties of materials over a wide frequency range. Such a goal can be achieved only by simplifying and speeding up processing of the experimental data. Therefore, the objective included not only the harware of a time domain experimental system but also the development of a software for such a system.

The electrical quantities describing dielectric materials

are introduced in Chapter 2 of this thesis while Chapter 3 reviews measuring techniques and methods for investigating such materials at high and microwave frequencies. Experimental planning is discussed in Chapter 4. Chapter 5 includes the design and development of the experimental system while Chapter 6 is devoted to the system software. The experimental verification of the system is presented in Chapter 7 of this thesis. The conclusions are discussed in Chapter 8.

CHAPTER 2

INTRODUCTION TO THE THEORY OF DIELECTRICS

Dielectrics include a broad expanse of nonmetals considered from the standpoint of their interaction with electric, magnetic, or electromagnetic fields. Thus we are concerned with the storage of electric and magnetic energy as well as with its dissipation. The macroscopic description of dielectrics and explanation of the phenomenon of dielectric polarization is discussed in this chapter.

2.1. Macroscopic Description of Dielectrics

The a-c characteristics of materials are best defined in terms of electromagnetic field concepts /1/. Basic to any discussion of the interaction of electromagnetic waves and matter are Maxwell's equations

$$\nabla \times \vec{E} = -j\omega\vec{B} \qquad \nabla\cdot\vec{B} = 0$$

$$\nabla \times \vec{H} = j\omega\vec{D}+\vec{J} \qquad \nabla\cdot\vec{D} = Q \qquad /2.1/$$

and the associated constitutive relationships

$$\vec{D} = \varepsilon\vec{E}$$

$$\vec{B} = \mu\vec{H}$$

$$\vec{J} = \sigma_c\vec{E} \qquad /2.2/$$

where $\vec{E}$, $\vec{H}$, $\vec{D}$, $\vec{B}$ and $\vec{J}$ are complex vector quantities of rms values and $e^{j\omega t}$ dependence, i.e., time-harmonic functions. $\vec{E}$ represents the electric field intensity, $\vec{H}$ the magnetic field intensity, $\vec{D}$ the electric flux density /or dielectric displacement/, $\vec{B}$ the magnetic flux density/or magnetic induction, $\vec{J}$ the electric current density, and $\vec{Q}$ is the electric charge density, a scalar quantity. ε, μ, and σ_c represent the complex a-c constitutive parameters of the material, which are the permittivity, the permeability, and the conductivity associated with conduction current, respectively. The free space constants μ_o and ε_o have respective values of $4\pi \times 10^{-7}$ henry/m and 8.85419×10^{-12} farad/m. Conductivity of free space is zero.

For most materials other than ferromagnetic substances, μ has essentially the value of μ_o. This holds true for biological materials and agricultural products. The permittivity is expressed as

$$\varepsilon = \varepsilon' - j\varepsilon'' = |\varepsilon| e^{-j\delta} \qquad /2.3/$$

The real part of the permittivity, ε', is called the dielectric constant. ε'' is the dielectric loss factor, and the angle δ is the dielectric loss angle. The value

$$\tan \delta = \frac{\varepsilon''}{\varepsilon'} \qquad /2.4/$$

is called the loss tangent or dissipation factor of the material.

In most practical work the dielectric properties of materials are related to the dielectric properties of vacuum or free space. The relative permittivity, relative dielectric constant, relative loss factor, and loss tangent are related as follows:

$$\varepsilon_r = \frac{\varepsilon}{\varepsilon_o} = \frac{\varepsilon'}{\varepsilon_o} - j\frac{\varepsilon''}{\varepsilon_o} = \varepsilon_r' - j\varepsilon_r'' = \varepsilon_r'(1-\tan\delta) \quad /2.5/$$

$$\tan\delta = \frac{\varepsilon_r''}{\varepsilon_r'} \quad /2.6/$$

The conductivity σ_c may be written as

$$\sigma_c = \sigma_c' + j\sigma_c'' \quad /2.7/$$

Substituting expressions 2.2 and 2.3 in the expression for the curl of $\vec{H}$ of Eqs. 2.1, we may write

$$\nabla \times \vec{H} = j\omega(\varepsilon' - j\varepsilon'')\vec{E} + (\sigma_c' + j\sigma_c'')\vec{E} = [j(\omega\varepsilon' + \sigma_c'') + \omega\varepsilon'' + \sigma_c']\vec{E} \quad /2.8/$$

The term $j\omega\varepsilon\vec{E} = j\omega(\varepsilon' - j\varepsilon'')\vec{E}$ represents the displacement current, while $\sigma_c\vec{E}$ represents the conduction current. Normally σ_c'' is negligible. The currents of Eq. 2.8 may also be considered as shown in the right-hand member where $(\omega\varepsilon'' + \sigma_c')\vec{E}$ represents a dissipative current in phase with $\vec{E}$ and $j(\omega\varepsilon' + \sigma_c'')\vec{E}$ represents a reactive current out of phase with $\vec{E}$. Generally, in dielectrics work the dissipative current is attributed to the dielectric loss, and the influence of the σ_c' component is lumped with the ε'' component so that the total loss current is considered to be $\omega\varepsilon''\vec{E}$. An a-c conductivity for the material equivalent to $\omega\varepsilon''$ can be calculated as

$$\sigma = \omega\varepsilon'' = \omega\varepsilon_0\varepsilon_r'' \qquad /2.9/$$

The relationships of Eqs. 2.5, 2.6, and 2.9 may also be derived from equivalent-circuit concepts, where a dielectric material is represented for a given frequency by a parallel-equivalent capacitance and resistance /3/. These concepts are applied in many measurement techniques where the dielectric properties are calculated from impedance or admittance measurements on dielectric material samples.

2.2. Microscopic Mechanisms of Polarization

Matter, electrically speaking, consists of positive atomic nuclei surrounded by negative electron clouds. Upon the application of an external electric field the electrons are displaced slightly with respect to the nuclei; induced dipole moments result and cause the so-called electronic polarization of materials /3/. When atoms of different types form molecules, they will normally not share their electrons symmetrically, as the electron clouds will be displaced eccentrically toward the stronger binding atoms. Thus atoms acquire charges of opposite polarity, and an external field acting on these net charges will tend to change the equilibrium positions of the atoms themselves. By this displacement of charged atoms or groups of atoms with respect to each other, a second type of induced dipole moment is created. It represents the atomic polarization of the dielectric. The

asymmetric charge distribution between the unlike partners of a molecule gives rise, in addition, to permanent dipole moments which exist also in the absence of an external field. Such moments experience a torque in an applied field that tends to orient them in the field direction. Consequently, an orientation or dipole polarization can arise. These three mechanisms of polarization are due to charges that are locally bound in atoms, in molecules, or in the structures of solids and liquids. In addition, charge carriers usually exist that can migrate for some distance through the dielectric. When such carriers are impeded in their motion, either because they become trapped in the material or on interfaces, or because they can not be freely discharged or replaced at the electrodes, space charges and a macroscopic field distortion result. Such a distortion appears as an increase in the capacitance of the sample. This mechanism of polarization is called space-charge or interfacial polarization.

Each of these four mechanisms of polarization takes place in a different frequency range. Therefore, for different frequencies of the applied alternating field, a different mechanism may dominate. Resonance effects, due to rotations or vibrations of atoms, ions or electrons /electronic and atomic mechanisms of polarization/ are noticed in the infrared, visible and ultraviolet regions, in the neighbourhood of the characteristic absorption frequencies. The space-

charge polarization is usually dominant in the low frequency regions, whereas the dipole polarization can be observed in the radio and microwave regions.

2.3. Polarization at High Frequencies

As frequency increases from low values, the polar molecules can follow the changes in direction of the electric field up to a point, and, as the frequency continues to increase, the dipole motion can no longer keep up with the changing field. As a result, the dielectric constant drops with increasing frequency in this region and energy is absorbed as a result of the phase lag between the dipole rotation and the field. At higher frequencies, the dielectric constant again levels off at the so-called optical value and the loss factor again drops to a low value, (Fig. 2.1).
Debye /1929/ developed the mathematical formulation which can be expressed as

$$\varepsilon_r = \varepsilon'_{r\infty} + \frac{\varepsilon'_{rs} - \varepsilon'_{r\infty}}{1 + j\omega\tau} \qquad /2.10/$$

Separating this into its real and imaginary parts yields

$$\varepsilon'_r = \varepsilon'_{r\infty} + \frac{\varepsilon'_{rs} - \varepsilon'_{r\infty}}{1 + \omega^2\tau^2} \qquad /2.11/$$

$$\varepsilon''_r = (\varepsilon'_{rs} - \varepsilon'_{r\infty}) \frac{\omega\tau}{1 + \omega^2\tau^2}$$

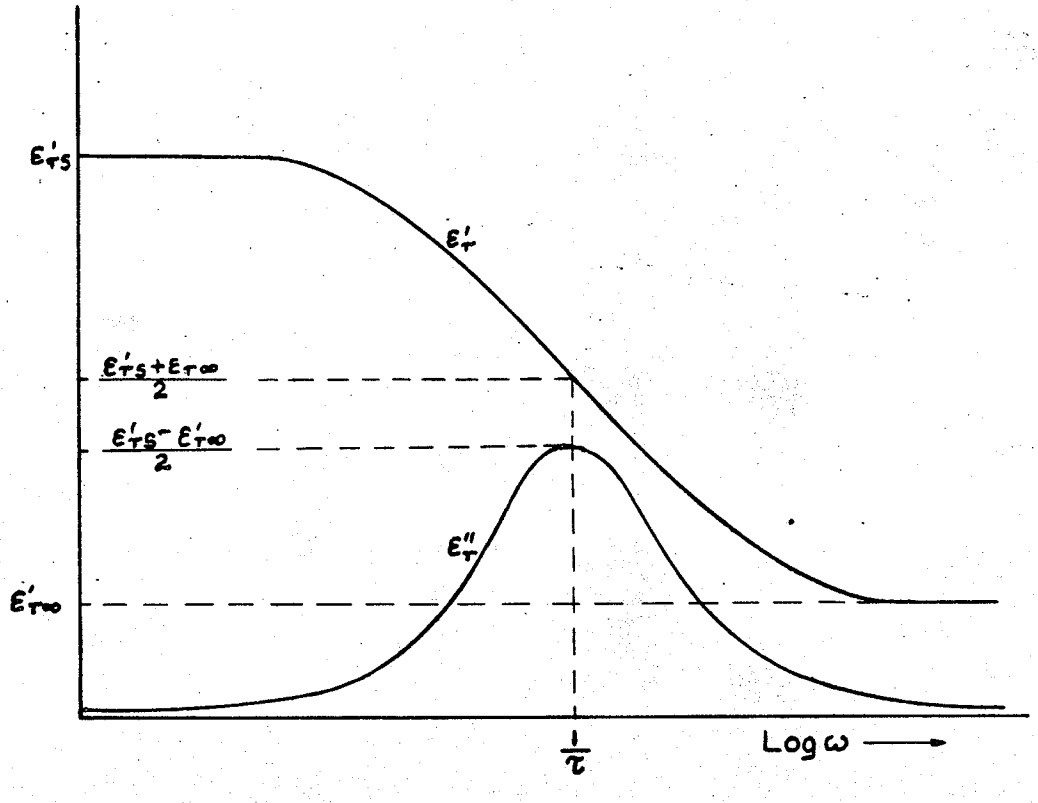

Fig.2.1. Dispersion and absorption curves for a polar material following the Debye relaxation process /1/.

where ε'_{rs} is the static or d-c value of the dielectric constant, $\varepsilon'_{r\infty}$ is the infinite - frequency or optical value, and τ is the relaxation time, the period associated with the time for the dipoles to revert to random orientation. Since the loss decreases to zero at the frequency extremes, $\varepsilon'_{rs}=\varepsilon_{rs}$ and $\varepsilon'_{r\infty}=\varepsilon_{r\infty}$, the prime notation on ε_{rs} and $\varepsilon_{r\infty}$ are often omitted.

It was noted by Cole and Cole that plotting ε'_r and ε''_r in the complex plane, in accordance with the Debye relation, results in a semicircle /Fig.2.2./. Eqs. 2.11 are parametric equations of a circle, and combining the two equations and eliminating $\omega\tau$ provides the following Cole-Cole relation:

$$\left(\varepsilon'_r - \frac{\varepsilon'_{rs}+\varepsilon'_{r\infty}}{2}\right)^2 + \left(\varepsilon''_r\right)^2 = \left(\frac{\varepsilon'_{rs}-\varepsilon'_{r\infty}}{2}\right)^2 \qquad /2.12/$$

This describes a circle of radius $\frac{\varepsilon'_{rs}-\varepsilon'_{r\infty}}{2}$ with center on the ε'_r axis at $\left(\frac{\varepsilon'_{rs}+\varepsilon'_{r\infty}}{2}, 0\right)$.

2.3.1. Distribution of relaxation times

In a condensed phase of a material the conditions for each molecule are strongly variable; the magnitude of interaction forces, directing force, and a thermal influence, all vary from place to place and from time to time. Every dipole in its own situation has at any moment its own intrinsic relaxation time. When an average is taken over spatial conditions, a spread of relaxation times generally results, distributed

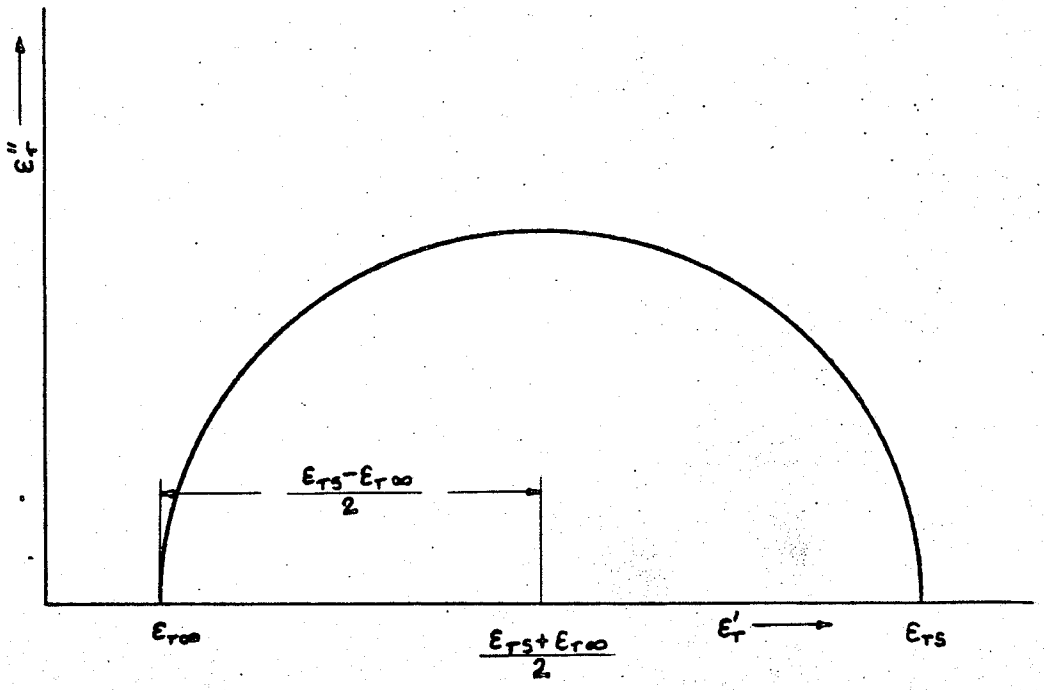

Fig.2.2. The relationship between ε''_r and ε'_r , according to the Debye relation /4/.

around the most probable value.

There is no satisfactory general theory describing the frequency dependence of ε_r' and ε_r'' in case of distributed relaxation times. Therefore, several authors tried to approach the problem from the empirical side. Cole and Cole /1941/ showed that in the case of distributed relaxation times, formula 2.10 must be modified to

$$\varepsilon_r = \varepsilon_{r\infty}' + \frac{\varepsilon_{rs}' - \varepsilon_{r\infty}'}{1 + (j\omega\tau)^{1-h}} \qquad /2.13/$$

which results in a Cole-Cole plot which is an arc of a circle with centre $\left(\frac{\varepsilon_{rs}' + \varepsilon_{r\infty}'}{2}, -\frac{\varepsilon_{rs}' - \varepsilon_{r\infty}'}{2} \operatorname{catan} \frac{(1-h)\pi}{2} \right)$ and radius $\frac{\varepsilon_{rs}' - \varepsilon_{r\infty}'}{2} \operatorname{cosec} \frac{(1-h)\pi}{2}$, as shown in Fig. 2.3. The Cole-Cole representation has been found to describe reasonably well the frequency dependence of the permittivity of some biological substances.

Several other models have been developed to explain the behavior of certain types of materials. One known as the Cole-Davidson representation results in a skewed arc, Fig.2.4, rather than the symmetrical Cole-Cole circular arc. The Cole-Davidson representation is defined as

$$\varepsilon_r' = \varepsilon_{r\infty}' + \frac{\varepsilon_{rs}' - \varepsilon_{r\infty}'}{(1 + j\omega\tau)^{\beta}} \qquad /2.14/$$

where β is restricted to values between 0 and 1. For $\beta = 1$ the arc is the Debye semicircle, but for values of $\beta < 1$

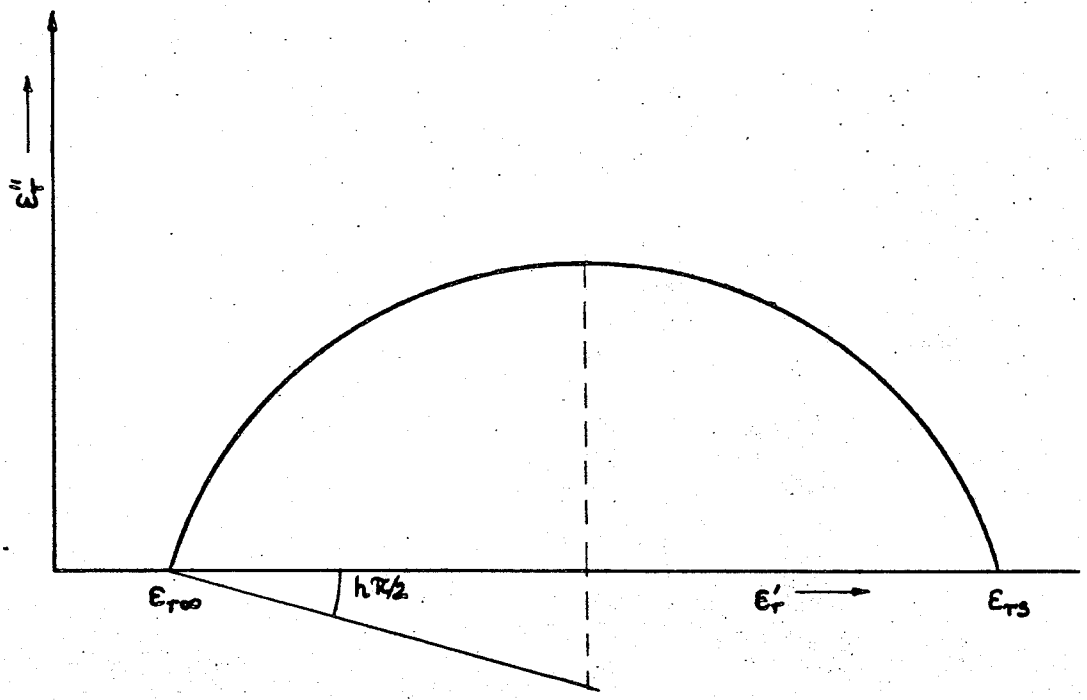

Fig.2.3. The Cole-Cole representation of ε'_τ and ε''_τ in the case of distributed relaxation times /5/.

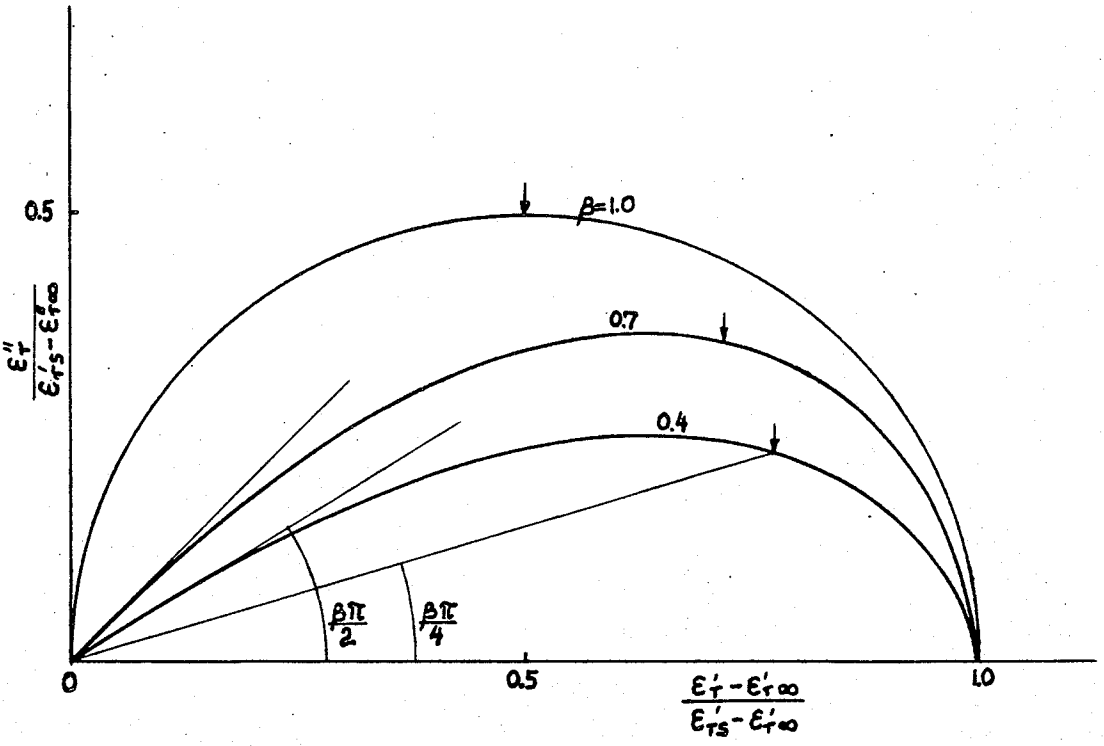

Fig.2.4. The Cole-Davidson representation of ε'_τ and ε''_τ ; the short arrows show where $\omega=\frac{1}{\tau}$ /4/.

the arc is skewed to the right. The Cole-Davidson representation is useful for materials exhibiting a nonsymmetrical distribution of relaxation times with polarization processes of decreasing importance extending into the higher frequency region.

A mathematical description of experimental data is much more complicated when two or more relaxation effects are overlapping. In this case, each dispersion is described by a different set of parameters and the resultant curve is obtained by a geometrical construction.

CHAPTER 3

DIELECTRIC MEASURING TECHNIQUES AND METHODS

Measurements of the dielectric properties of materials can be made either in the time domain or the frequency domain. For convenience, methods and techniques for these two domains are reviewed separately. The limits of frequency ranges are arbitrary and have been selected only for the purpose of this thesis.

3.1 Frequency Domain Methods

Neither the dielectric constant nor the loss factor of a test material are determined directly; the parameters which are measured depend on the frequency. In the medium frequency range, the capacitance and the dissipation factor of a dielectric sample are measured by the null method /6/, involving some type of a capacitance bridge. The dielectric constant and loss factor are calculated therefrom. At higher frequencies the errors of the capacitance bridge method become excessive and therefore a resonant circuit is usually used for measurements. The capacitance of the sample is measured by the substitution method, but the loss component is found from the width of the resonance curve. In the microwave frequency range, lumped circuits can no longer be utilized and typical distributed element techniques are employed in measurements. The

high and microwave frequencies are of interest in this research.

3.1.1. High frequency range /100 kHz to 300 MHz/

In this frequency range, resonant circuits are used with resonance indicated by a high input impedance voltmeter. The dissipation factor of the circuit is usually obtained from the width of the resonance curve, determined by either susceptance or frequency variation /6/. The lower frequency limit /ca. 10 kHz/ is given by the input resistance of the voltmeter. An upper limit /ca. 300 MHz/ is set by the smallest inductor that can be built with a sufficiently low dissipation factor, since the tuning capacitance must be somewhat larger than that of the dielectric sample. Additional limitations are imposed by the dimensions of the sample and its electrodes which must be very small compared to the wavelength and by the radial resistance of the foil electrodes applied to the dielectric.

3.1.2. Microwave frequency range /300 MHz - 200 GHz/

Microwave measuring techniques are employed to determine the dielectric properties of materials in this frequency range. Transmission lines /both waveguides and coaxial/,

sloted lines, microwave bridges, resonant cavities and other distributed elements are used rather than lumped elements and circuits. Neither the dielectric constant nor the loss factor are determined directly but they are calculated from the input impedance, reflection or transmission coefficients and the parameters of resonant cavities /7/..

There are three groups of methods for measuring the permittivity at microwave frequencies /2/, /6/. These are the reflection, transmission and perturbation methods. The most popular method is the first group which is based on measurements of the input impedance of a sample, open and short-circuited at its far end. The method is usually used with samples inserted into waveguide or coaxial lines. Another method in this group is the very-long-sample method, which is based on measurements of the input impedance of a relatively long sample so that the reflections from its far end can be neglected. A modified version of this method has been developed /8/ which allows measurements over a relatively wide frequency range even for dielectrics in granular and powdered form and relatively short samples.

Transmission methods, which are based on measurements of the complex transmission coefficient of the sample in the waveguide or coaxial line, are less popular because of the complicated measuring arrangements required and lower accuracy obtainable.

Perturbation methods are based on measurements of the incremental changes in the resonance frequency and Q-factor of a resonant cavity containing a very small sample of the test material. Nowadays these methods are intensively investigated since the parameters of the cavity can be controled automatically by an electronic circuitry. The applications of these methods for measuring dielectric properties of liquids flowing through an open-ended cavity have been reported /9/, /10/.

3.2. Time Domain Dielectric Spectroscopy

Since about 1969 transient methods have been used in the study of fast relaxation processes. All the transient methods originate from a technique called Time Domain Reflectometry /TDR/. Presently, not only the reflection methods but also the transmission methods are used to investigate the dielectric properties of materials. Therefore, all transient methods are collectively called Time Domain Spectroscopy /TDS/ methods. The accuracy of TDS methods is at present comparable to that of standard frequency domain methods. Striking advantages are the simple equipment needed /a sampling oscilloscope/ and the relatively short time required to do the measurements. At present the frequency range covered by these methods is from the kHz region up to about 15 GHz /11/.

In all time domain methods a fast-rise-time step volt-

age is propagated in a low loss coaxial line. This step voltage is detected at the "sampling head" of the sampling system and displayed /after being transformed to a longer time scale/ on an oscilloscope. The step voltage is also travelling to the dielectric sample enclosed and all reflected voltages which reach the sampling head at some later time are also displayed on the oscilloscope screen.

Obviously it is possible to select specific phenomena /as the reflection behaviour against one interface only/ within a specific "time window". Other, unwanted, phenomena /as reflections from the second interface/ then occur outside the time window and therefore do not disturb the measurement. Experimentally this property is used to diminish the influence of unwanted reflections from connectors, sampler, sampling head, etc.

The permittivity of the test material can be found by Fourier analysis of both the incident and reflected signals. All computations necessary in the processing of experimental data are done by digital computers.

To conclude this chapter, a comparison is given in Table 3.1 between the TDS and frequency domain techniques /12/.

Table 3.1

Comparison between time domain and frequency domain methods

Frequency range 10 MHz to 10 GHz

Time Domain Methods	Frequency Domain Methods
Relatively inexpensive equipment /e.g. HP 1815/1817, 35 ps TDR system - about $ 4250 in 1974/	Expensive equipment /e.g. HP 8410/8620, 110 MHz to 2 GHz Network Analyzer - about $ 16 000 in 1974/
Measurements not time consuming at microwave frequencies /about 5 minutes/	Time consuming experiments at microwave frequencies /several hours for traditional techniques but several minutes for Network Analyzer/
Accuracy comparable with frequency domain methods $\frac{\Delta\varepsilon_0}{\varepsilon_0} \simeq 5\%$, $\frac{\Delta\varepsilon_\infty}{\varepsilon_\infty} \simeq 20\%$, $\frac{\Delta\tau}{\tau} \simeq 7.5\%$	$\frac{\Delta\varepsilon_0}{\varepsilon_0} \simeq 1\%$, $\frac{\Delta\varepsilon_\infty}{\varepsilon_\infty} \simeq 10\%$, $\frac{\Delta\tau}{\tau} \simeq 7.5\%$
High frequency limit, in principle due to the finite rise time of the step voltage and time reference procedure /in practice $f < 10$GHz/	No high frequency limit a priori /in practice $f < 40$ GHz in guided systems/

Time Domain Methods	Frequency Domain Methods
Low frequency limit due to the necessity to obtain a "complete" time domain curve /in practice $f > 10$ MHz/	No low frequency limit a priori but different techniques must be used when frequency decreases
Indirect estimation of ε' and ε'' from Fourier analysis	ε' and ε'' calculated from electrical parameters
Calculator or computer is necessary	Calculator or computer not necessary in principle but needed in practice
The influence of errors, involved in the measurement, is spread out over all frequencies	Any error involved in measurement gives an error in ε' and ε'' for one frequency only /provided that the error is not systematic/

CHAPTER 4

EXPERIMENTAL PLANNING

Measurements of the dielectric properties of materials in the time domain offer many advantages as discussed in section 3.3. The measurements can be done by employing different methods and techniques. A lumped capacitance method was utilized in this research because of its inherent advantages such as speed, simplicity, relative ease of data evaluation and the very small sample required.

4.1. Measurement Method

In the lumped capacitance method /13-15/ a small shunt capacitor terminating a coaxial line section is used as a sample holder as shown in Fig. 4.1 /a/. An equivalent circuit of the sample holder is shown in Fig. 4.1 /b/, where ε_r is the relative permittivity of the substance filling the test capacitor. The permittivity can be calculated from the measured input reflection coefficient of the sample holder. The reflection coefficient at the A-A plane for the transmission line section terminated by a load impedance is $Z_L(\omega) = \frac{1}{j\omega C(\omega)}$ is

$$\Gamma = |\Gamma| e^{-j\theta} = \frac{1 - j\omega C_0 Z_0 \varepsilon_r}{1 + j\omega C_0 Z_0 \varepsilon_r} \qquad /4.1/$$

The real and imaginary parts of the relative permittivity may be found directly from /4.1/ in the form

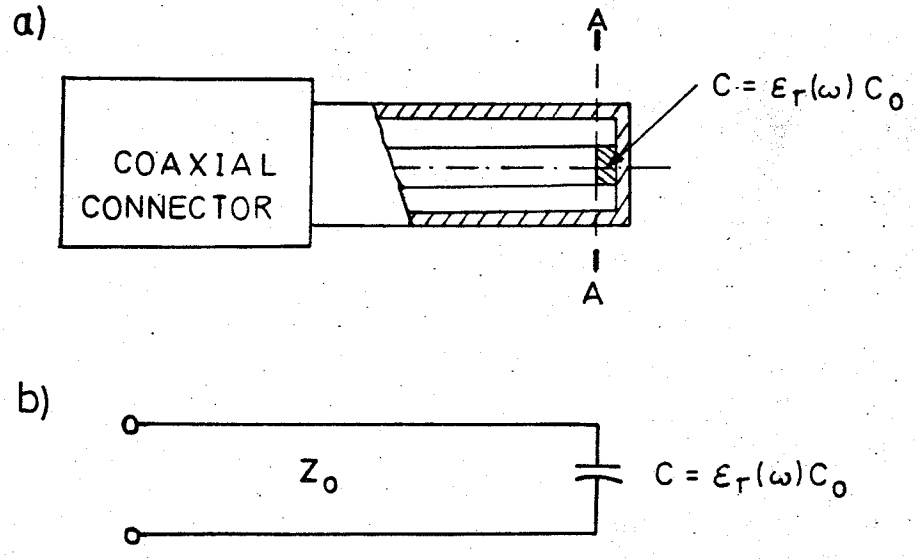

Fig.4.1. /a/ Coaxial sample holder and /b/ its equivalent circuit.

$$\varepsilon_r' = \frac{2|\Gamma|\sin\theta}{\omega C_0 Z_0 (|\Gamma|^2 + 2|\Gamma|\cos\theta + 1)} \qquad /4.2/$$

$$\varepsilon_r'' = \frac{1 - |\Gamma|^2}{\omega C_0 Z_0 (|\Gamma|^2 + 2|\Gamma|\cos\theta + 1)} \qquad /4.3/$$

By knowing the frequency dependence of the input reflection coefficient, the frequency dependence of ε_r' and ε_r'' can be found. The input reflection coefficient can be calculated from the time response of the capacitor to an incident step voltage applied to the sample holder, i.e.

$$V_r(t) = V_{in}(t) * \Gamma(t) \qquad /4.4/$$

where $V_{in}(t)$ and $V_r(t)$ are the incident and reflected waves respectively and * denotes convolution. The frequency dependence of the input reflection coefficient can be found by taking the ratio of the Fourier transforms of both waves, i.e.,

$$\Gamma(\omega) = \frac{F V_r(t)}{F V_{in}(t)} \qquad /4.5/$$

The detailed uncertainty analysis has been given in /13-15/ and it has been shown that

$$\frac{\partial \varepsilon'}{\partial C_0} = \frac{2|\Gamma|\sin\theta}{\omega C_0^2 Z_0 \{(|\Gamma|\cos\theta + 1)^2 + |\Gamma|^2 \sin^2\theta\}} \qquad /4.6/$$

$$\frac{\partial \varepsilon'}{\partial Z_0} = \frac{2|\Gamma|\sin\theta}{\omega C_0 Z_0^2 \{(|\Gamma|\cos\theta + 1)^2 + |\Gamma|^2 \sin^2\theta\}} \qquad /4.7/$$

$$\frac{\partial \varepsilon'}{\partial |\Gamma|} = \frac{2(1 - |\Gamma|^2)\sin\theta}{\omega C_0 Z_0 \{(|\Gamma|\cos\theta + 1)^2 + |\Gamma|^2 \sin^2\theta\}^2} \qquad /4.8/$$

$$\frac{\partial \varepsilon'}{\partial \theta} = \frac{2|\Gamma|\{(1+|\Gamma|^2)\cos\theta + 2|\Gamma|\}}{\omega C_o Z_o \{(|\Gamma|\cos\theta + 1)^2 + |\Gamma|^2 \sin^2\theta\}^2} \qquad /4.9/$$

$$\frac{\partial \varepsilon''}{\partial C_o} = -\frac{1-|\Gamma|^2}{\omega C_o^2 Z_o \{(|\Gamma|\cos\theta + 1)^2 + |\Gamma|^2 \sin^2\theta\}} \qquad /4.10/$$

$$\frac{\partial \varepsilon''}{\partial Z_o} = -\frac{1-|\Gamma|^2}{\omega C_o Z_o^2 \{(|\Gamma|\cos\theta + 1)^2 + |\Gamma|^2 \sin^2\theta\}} \qquad /4.11/$$

$$\frac{\partial \varepsilon''}{\partial |\Gamma|} = -\frac{2\{2|\Gamma| + (1+|\Gamma|^2)\cos\theta\}}{\omega C_o Z_o \{(|\Gamma|\cos\theta + 1)^2 + |\Gamma|^2 \sin^2\theta\}^2} \qquad /4.12/$$

$$\frac{\partial \varepsilon''}{\partial \theta} = \frac{2|\Gamma|(1-|\Gamma|^2)\sin\theta}{\omega C_o Z_o \{(|\Gamma|\cos\theta + 1)^2 + |\Gamma|^2 \sin^2\theta\}^2} \qquad /4.13/$$

The uncertainties ΔC_o and ΔZ_o result from the uncertainties in length measurement. For modern coaxial components these can be assumed to equal 0,1 percent. An additional uncertainty in determination of C_o results from the presence of the fringing field effects and the meniscus of the test liquid, but these are very difficult to evaluate. The uncertainties $\Delta|\Gamma|$ and $\Delta\theta$ are caused by the noise-like errors in the TDS system and by the time-to-frequency conversion errors /16/.

4.2. Typical Experimental Setup

A block diagram of a typical experimental setup is illustrated in Fig. 4.2. The experimental setup is shown in simplified form to clearly indicate the interconnection of the essential parts: a step function generator, sampling head, sampling oscilloscope, X-Y recorder and a sample holder.

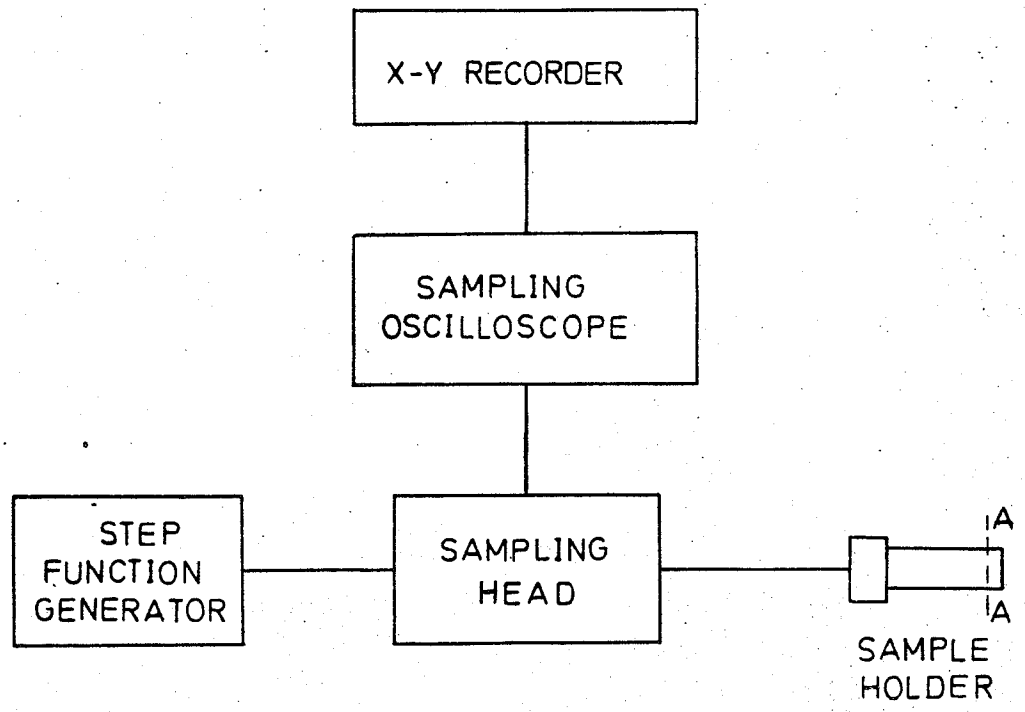

Fig.4.2. Typical experimental setup.

A tunnel-diode pulse generator produces very fast step pulses /rise time of approximately 20 psec for Hewlett-Packard model 1106A pulse generator mount/ which are used as excitation of the sample holder.

A remote sampler containes sample and hold circuit used for sampling incident and reflected pulses. It also provides bias and trigger signals for operating the tunnel-diode pulse generator. The sampling oscilloscope with the TDR plug-in provides drive voltages for the oscilloscope horizontal amplifiers to position each sample dot on the screen of the CRT. In vertical channel the TDR takes samples /through the sampling head/ of the incoming signals and supplies the drive voltages to the oscilloscope vertical amplifiers. In addition the TDR plug-in provides control signals for the remote sampler and blanking pulses for the oscilloscope. The CRT displays are recorded on an X-Y recorder using horizontal and vertical signals available at the output of the oscilloscope.

The recorded waveforms are then analyzed manually and Fourier transforms are calculated using a digital computer. The relative permittivity of the test material ε_r is then calculated from Eqs. /4.2/ and /4.3/.

Uncertainties of 1.4 percent in $\Delta|\Gamma|$ and 0.8° in $\Delta\theta$ were reported /13/ for a Hewlett-Packard experimental setup consisting of an HP 180 D oscilloscope, HP 1815 TDR plug-in,

HP 1817A TDR sampler and an HP 1106 A tunnel-diode generator mount.

The measuring method and equipment used are very fast but the extraction of information from the recorded waveforms slows down measurements and limits the achievable accuracies. It was the object of this research to develop a system which would speed up measurements and eliminate manual data processing.

CHAPTER 5

DESIGN AND DEVELOPMENT OF THE EXPERIMENTAL SYSTEM

The design and development of a system for time-domain measurements of the dielectric properties of materials require consideration of many different aspects. The system should provide fast measurements, an easy calibration procedure and easy data processing. Recording of the waveforms and manual analysis of the experimental results should be avoided. Further, the system should be characterized by simplicity of operation, reliability and accuracy and its output should be computer compatible. Existing or commercially available equipment should be utilized in the system wherever possible.

5.1. Block Diagram of the System

A simplified block diagram of the system which has been developed to cope with the above-listed requirements is shown in Fig. 5.1.

A step voltage produced by the TDR system is applied to the sample of a test material placed into the sample holder. The incident wave and the wave reflected by the test substance are sampled by the TDR and displayed on the screen of the sampling oscilloscope after being transformed to an expanded time scale. All necessary adjustments can be made

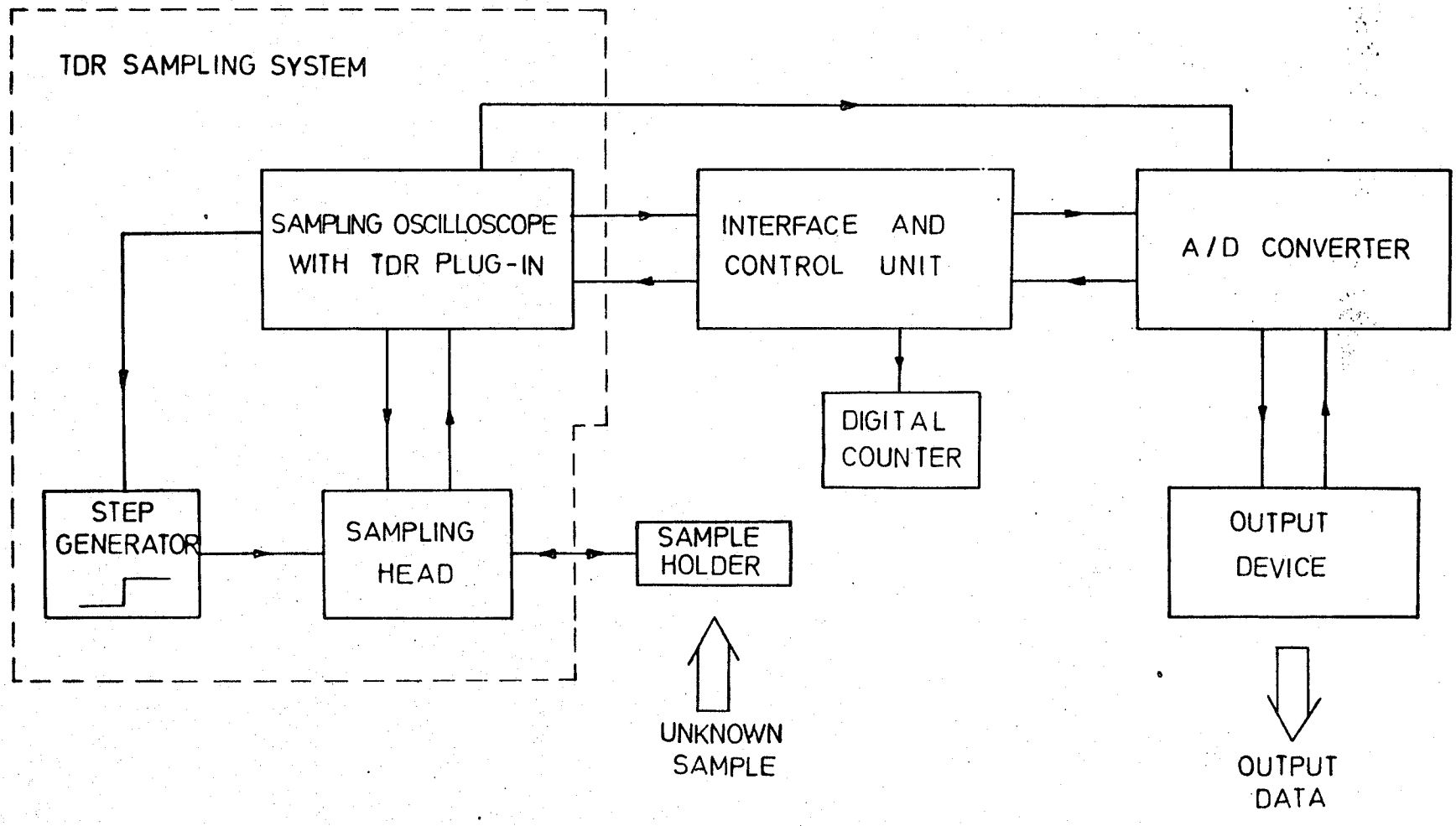

Fig.5.1. The simplified block diagram of the experimental system.

in this mode of operation. Then the TDR system is set to the "record" mode of operation and the output voltage of the oscilloscope vertical amplifier /which is proportional to the excitation and response/ is digitized by an analog to digital converter. All signals necessary for the converter are supplied by the interface and control unit. The output signals from the analog to digital converter /in BCD code/ are fed to an output device which produces the output data of the system in a form depending on the type of device used. In a Hewlett-Packard Model 5055A Digital Recorder, the output data is printed on paper tape. In addition, a digital counter /Monsanto, Model 105 A/ is used in the system for counting the samples taken during a measurement cycle.

It should be pointed out thal all the controls are performed automatically by the interface and control unit and, therefore, the operation of the system is as simple as the use of the TDR system.

5.2. Sample Holder

An APC-7 precision sample holder has been designed. A commercially available APC-7 precision connector was utilized in the sample holder, whereas the precision coaxial air line and the cap /Fig. 5.2/ were manufactured.

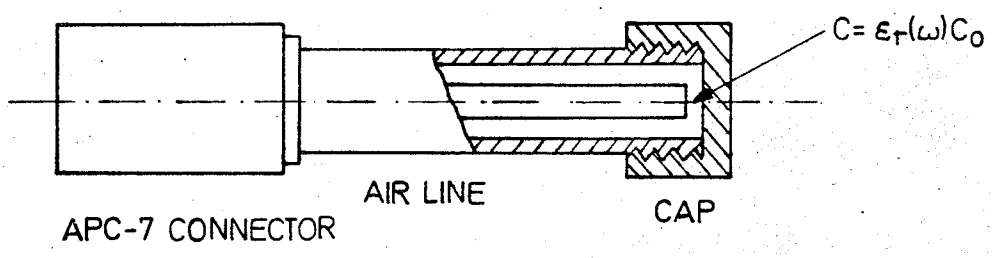

Fig.5.2. APC-7 precision sample holder.

The diameter of the inner conductor and the inner diameter of the outer conductor of the air line are 3.04038 $\pm$ 0.0025 mm and 7.00024 $\pm$ 0.0038 mm, respectively, which gives a characteristic impedance of the line $Z_o = 50\Omega \pm 0.2$ percent. In the lumped capacitance method it was shown elsewhere /14/ that there is an optimum value of capacitance C_o of an empty sample holder for a given dielectric at a given frequency. For lossless dielectrics / $\varepsilon''=0$ / the optimum value of capacitance C_o can be found from the relation

$$\frac{Z_c}{Z_o} = \varepsilon_r' \qquad (5.1)$$

where Z_c is the impedance of C_o.

The optimum capacitance of an empty sample holder for lossy dielectrics / $\varepsilon''\neq 0$ / can be determined from the relation

$$\frac{Z_c}{Z_o} = \left(\frac{Z_c}{Z_o}\right)_{\varepsilon''=0} \cdot \left(1 + \tan^2\delta\right)^{1/2} \qquad (5.2)$$

where $\tan\delta = \varepsilon_r''/\varepsilon_r'$ is the loss tangent of the test dielectric. The optimum values of C_o were calculated for many dielectric materials. Three values of the capacitance of an empty holder were chosen for the frequency range of 0.1 GHz to 10 GHz.

The following values of the capacitance of an empty sample holder can be obtained by changing the inner conductor:

1. C_o = 2.8261 pF, for dielectrics having $\varepsilon_r' \simeq 3$
2. C_o = 0.2923 pF, for dielectrics having $\varepsilon_r' \simeq 5 - 20$
3. C_o = 0.0339 pF, for dielectrics having $\varepsilon_r' \simeq 80$.

Thus only one sample holder can be used for measurements of dielectrics for the whole frequency range of interest.

5.3. TDR Sampling System

The Hewlett-Packard TDR system utilized in the experimental setup consists of a 180D oscilloscope with a 1815B TDR /sampling plug-in and a 1817A sampling head with a 1106A tunnel diode mount.

The tunnel diode mount generates step-like pulses of amplitude greater than 200 mV into a 50Ω line, with a rise time of approximately 20 ps. It has an output impedance of 50Ω ± 2%.

The sampling head has 28 ps rise time detacheable, remote, single channel, feed-through sampler for use in 50Ω transmission systems. The maximum safe input voltage is 1 volt.

The oscilloscope with the TDR plug-in combined with the remote sampler and the tunnel diode mount composes a calibrated TDR system which has a rise time less than 35 ps with an overshoots less than ± 5% and a time jitter less than 15 ps. A signal-averaging function is provided which reduces noise and jitter by a ratio of 2 : 1 or more and which does not degrade the system performance. At the rear panel of the oscilloscope the outputs for the vertical and horizontal signals are provided as well as the input of the Z-axis

oscilloscope amplifier which is used for external intensity modulation. The TDR plug-in generates itself a marker pulse which is supplied to the control grid of the CRT to intensify the presentation of one selected dot. In the TDR system, one sweep of the oscilloscope time-base takes approximately 40 ms except for the "record" mode of operation when one curve is drawn on the oscilloscope screen in approximately 60 seconds. This mode of operation is utilized in analog to digital conversion of displayed curves.

The following outgoing signals are used for combining the TDR with other parts of the experimental system:

1. Signal proportional to the output voltage of the vertical oscilloscope amplifier /from the oscilloscope rear-panel connector to the analog to digital converter/,
2. Time-base ramp voltage /from the time-base generator circuit of the TDR plug-in to the interface and control unit/,
3. Step voltage /from the marker comparator circuit of the TDR plug-in to the interface and control unit/,
4. Two level voltage signal /from the scan switch of the TDR plug-in to the interface and control unit/.

5.4. Analog to Digital Conversion

A Hewlett-Packard 3485A Scanning Unit with a 3480 A Digital Voltmeter were used as an analog to digital converter. The 3485A makes the 3480A Multifunction DVM into a scanner which includes its own signal conditioning, digitizing and BCD output. Scan modes include Step, Single Scan, Continuous Scan and Random. The dwell time on each channel may be varied from 1s to no delay in six steps. This allows the scanner to be used from 1channel/ second up to 1000 channels/second. Any one channel may be randomly addressed and successive readings may be made on that channel using the "Monitor" pushbutton or remote control signal. The scanner has three ranges: 100 mV, 1000 mV and 10V full scale with $> 10^7 \Omega$ input resistance to reduce loading errors. Autoranging is provided to simplify measurements over a wide range of amplitudes. Digitization includes 4 full digits plus a 5-th digit for 50% overranging. Common-mode voltage errors may be reduced by a guard available on each block of 10 channels. A 30 dB /at 60 Hz/ filter is available to limit normal-mode noise. Isolated Remote Control is provided for remote control of the scanner. All control signals are supplied by the interface and control unit of the experimental system, in which the scanner is utilized as analog to digital

converter. The "Step" and "Continuous Scan" modes of operation are utilized in this application of the scanner. Channel number one is remotely selected and, therefore, in the continuous mode of operation, the input curve is sampled continuously upon the manual or remote "Initiate" command. The digitization of the curve can be stopped by the manual or remote "Home" command. The sampling rate of this analog to digital conversion depends on the preselected channel delay and the output device used in the system. With a Hewlett-Packard Model 5055A Digital Recorder, the number of samples taken during 1 minute conversion time may be selected in the range of 60 to more than 600. In the "Step" mode of operation, each sample is taken upon a manual or remote command. An external clock can be used for remote control commands. The following remote command signals are supplied to the scanner by the interface and control unit:

Program Commands:

1. Mode Enable - selects one of the scan modes /4 lines/,
2. Range Enable - selects one of the 3 ranges /2 lines/,
3. Channel Select - selects channel using 7 BCD coded lines,

Control Commands:

4. Program Execute - causes the remote commands present on the program lines to be entered into the program storage,

5. Program Initiate - causes execution of a program entered into the program storage,
6. Home /Reset/ - returns the scanner to Home position /all channels open, input amplifier short-circuited/.

This is used to stop the analog to digital conversion. The scanner supplies two commands to the interface and control unit which are:

1. Program Acknowledgement-indicates that the program has been entered into storage by the Program Execute command,
2. Print Command - indicates that the digitization of the sample has been completed and the BCD output may be recorded.

5.5. Interface and Control Unit

The unit has been designed and built to interface the TDR system with the scanner and to provide a fully automatic analog to digital conversion of TDR responses. Besides the control of the experimental system, provision has been made for triggering the analog to digital converter by an external clock. In addition, the unit interfaces the scanner with an electronic counter which is used in the system for counting the samples taken during the analog to digital conversion. The "ready" state of the whole experimental system is indicated

by a red light on the front panel. The unit can also serve as an interface between the analog to digital converter and other equipment having an analog output /e.g., a low frequency time domain spectroscopy system/.

A block diagram of the interface and control unit is shown in Fig. 5.3., while the detailed schematic diagrams and the list of cable connections are given in appendices A and B, respectively.

A power supply has been built to provide the necessary voltages for transistors as well as for linear and digital integrated circuits used in the unit. In the digital part of the unit, the TTL integrated circuits have been used. Thus, in this part of the unit, signals can have two levels:

a/ low - 0V to less than 0.8 V /typically 0.2 V/,

b/ high - more than 2.0 V but less than 5 V /typically 3.3 V/.

The Initiate and Scan Switch Comparators and the Buffer Amplifier /G_u = 1/ have high input impedances /1.2MΩ, 21MΩ and 10.5MΩ, respectively/ to avoid disturbances in the normal operation of the TDR system.

In the state previous to the measurement cycle, the Scan Switch signal coming from the TDR has the value of 10 V and therefore the output of the Scan Switch Comparator is in the high state, which results in a low level of the limiter/inverter output. Thus, the Home signal has the low level and the scanner is in the reset position. The Time-Base signal of the TDR goes through the Buffer Amplifier and the Stop Marker

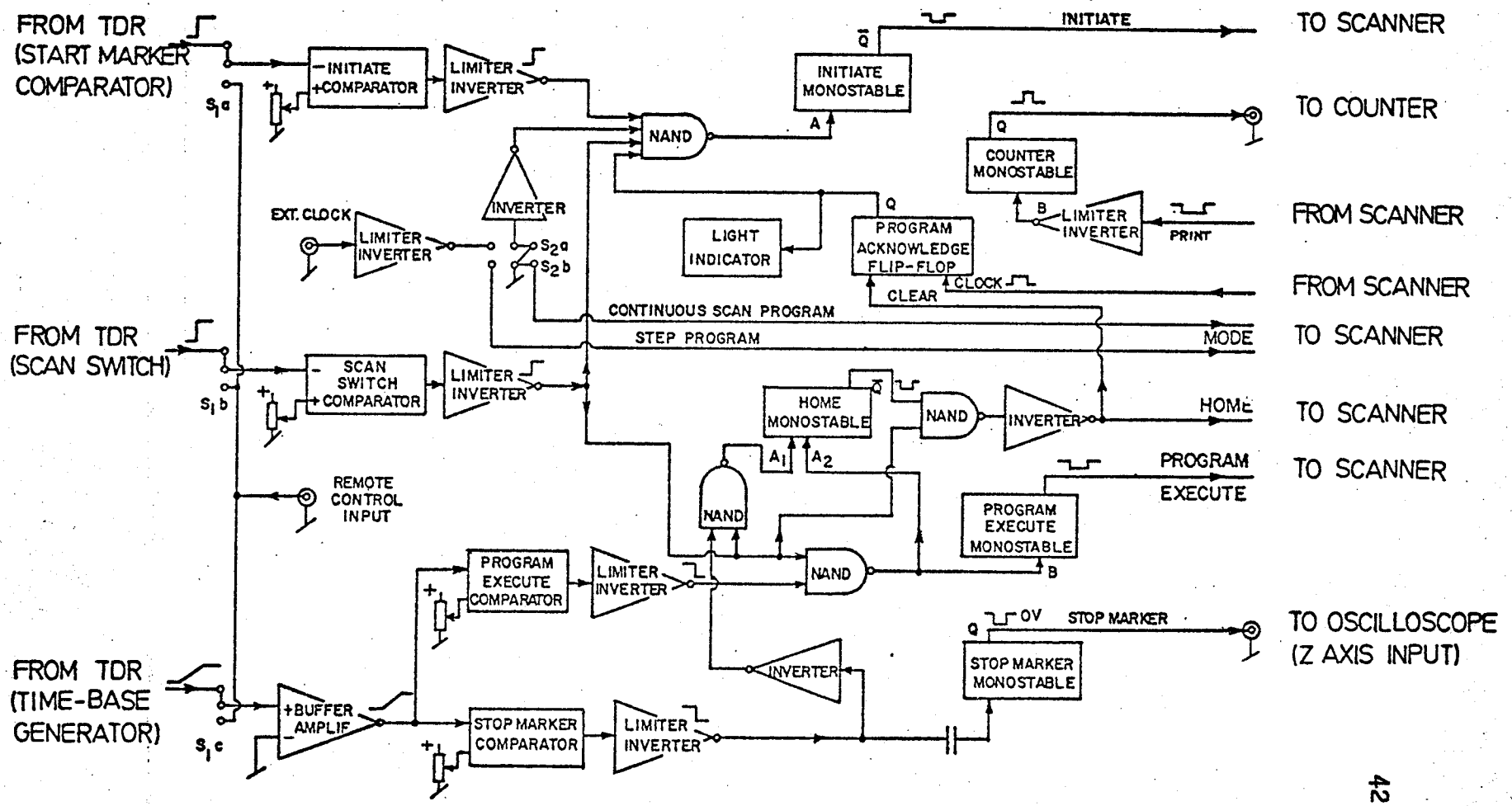

Fig.5.3. The block diagram of the interface and control unit.

Comparator compares it with the reference voltage. The output signal of the limiter/inverter triggers the Stop Marker Monostable Multivibrator which produces negative pulses used for the intensification of a dot on the TDR oscilloscope screen. This marker indicates the point at which the conversion will stop during the measurements.

During the measurement period the Scan Switch signal has the value of 100 V, and thus the output of the limiter/inverter has the high level and the locking low level of the Home signal is removed. At the beginning of the measurement period, the Program Execute Comparator produces the triggering pulse for the Program Execute Monostable Multivibrator /positive edge input/. The Program Execute signal causes the selected program to be entered into the scanner program storage. The scanner responses by the Program Acknowledgement signal which changes the output of the Program Acknowledgement Flip-Flop to the high level. The "ready" light goes on.

When the Start Marker signal coming from the TDR changes its level from 0 V to 15 V, the Initiate Comparator goes into action and the output of the limiter/inverter goes to the high level. The output of the NAND gate goes to the low level which triggers the Initiate Monostable Multivibrator /negative edge input/. The Initiate signal starts the analog to digital conversion. The Print signals coming from the scanner trigger the Counter Monostable Multivibrator /positi-

ve edge input/ which produces positive pulses. These pulses are counted by an electronic counter. The conversion lasts until the action of the Stop Marker Comparator, which through the limiter, inverter and NAND gate triggers the Home Monostable Multivibrator /negative edge input A_1/. The Home Monostable Multivibrator can also be triggered /negative edge input A_2/ by the Program Execute Comparator in the case when the conversion is stopped manually by setting the TDR Scan Switch to the reset position. The Home signal returns the scanner to the reset position. In addition, it changes the output of the Program Acknowledgement Flip-Flop to the low level which locks the Initiate NAND gate and causes the "ready" light to go off.

When the interface and control unit are to be used with an equipment other than the TDR system /the Control Switch in the remote position/, the high level should be applied to the Remote Control Input at least 2 ms prior to the measurement cycle. The removal of this signal will return the scanner to the reset position. The interface and control unit was thoroughly tested and was found very satisfactory in operation.

CHAPTER 6

PROCESSING OF THE EXPERIMENTAL DATA

Since the dielectric properties of a test material are not measured directly a calibration and normalization procedure is included in measurements and a digital computer is employed in data processing in order to find the permittivity of the test substance.

6.1 Calibration and Normalization Procedure

The calibration procedure consists of amplitude and time scale calibrations. For the amplitude scale calibration, the sample holder can be open ended or short circuited. The open ended case /Γ=1/ was utilized in the system for calibration and for measurements of the incident wave. In this case reflected wave has the shape of the incident wave, Fig. 6.1. The parameters which are necessary for the normalization of the system output data are evaluated by a digital computer as follows:

1. Reference level RPO, which corresponds to the zero value of the reflection coefficient, is calculated as an average value of the samples taken on the beginning flat part of the display,
2. Reference level RPS, which corresponds to the Γ=1, is calcualted as an average value of the samples taken on the latter flat part of the display,

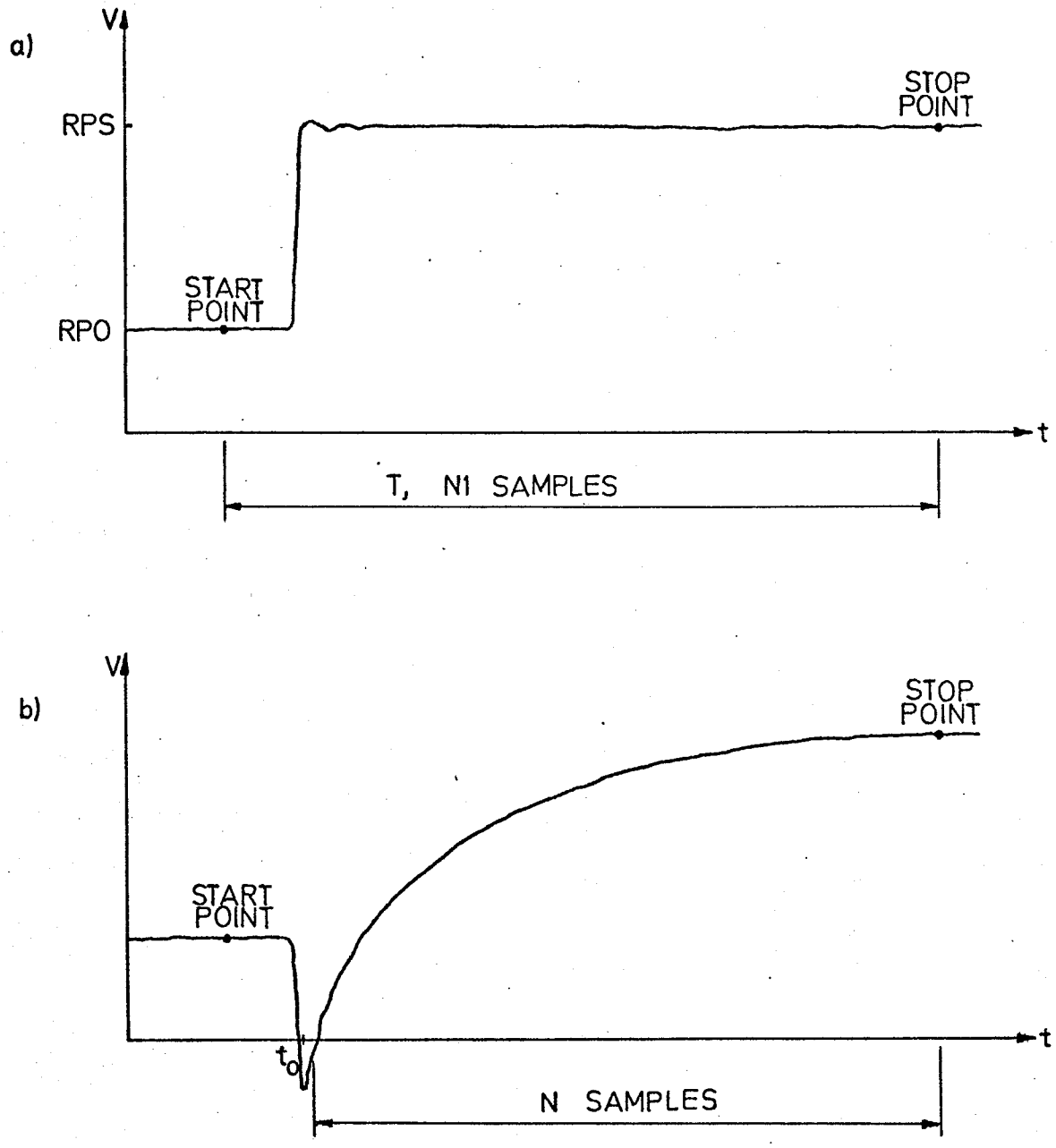

Fig.6.1. The displays of the TDR oscilloscope screen
/a/ the sample holder is open ended,
/b/ the sample holder is filled up with a test material.

3. The amplitude of the incident step wave, RFAC, is determined by subtracting these two levels.

When the values of the normalization parameters are known, the curves are normalized using the formula

$$V_n\,(n\Delta T) = \frac{V\,(n\Delta T) - RPO}{RFAC}$$

where $V/n\Delta T/$ is the measured value of the n-th sample. The time scale calibration consists of finding the time distance ΔT between two adjacent samples. If N1 samples are taken in the time window T between the Start and Stop points of the analog to digital conversion, then $\Delta T = T/N1$. The time window T is known from the TDR system while N1 is the reading of a digital counter used in the experimental system.

Only N successive samples, taken starting from the point t_o, Fig. 6.1. /b/, are used to describe the curves. The remaining N1-N samples are utilized for the calibration only, and they are neglected in the computations of the Fourier Transforms. The error involved in the determination of the time reference point to consists of the time jitter of the TDR system and the error introduced by the analog to digital conversion. Thus the total error is equal to $\tau_j + \frac{T}{2N1}$. This error can be decreased by increasing the number of samples N1 taken during the time window T. For the TDR time jitter $\tau_j = 15$ ps and for the typical values N1 = 500 and T = 2ns, the total error is estimated to be less than 17 ps.

6.2. Software for the Experimental System

Software for the system has been developed to perform all computations necessary for finding the permittivity of a test material by means of a digital computer. A flowchart of the software is shown in Fig. 6.2. while the computer program, written in WATFIV, is given in Appendix C. The flowchart is shown in simplified form to present basic principles of the software.

The program performs the following successive steps:

1. The values of the normalization parameters are found and printed out.
2. The name and the temperature of a test material are read and printed out.
3. The input control parameter NREF is read and printed out.
4. The proper values are set for array subscripts and program constants depending on the value of NREF. A value >0 prepares the computer for reading of the response signal, while 0 for reading of the excitation signal. A value <0 indicates that there is no more data available.
5. The input parameter KIND and the data for finding the Fourier Transform of the signal /excitation or response/ are read.

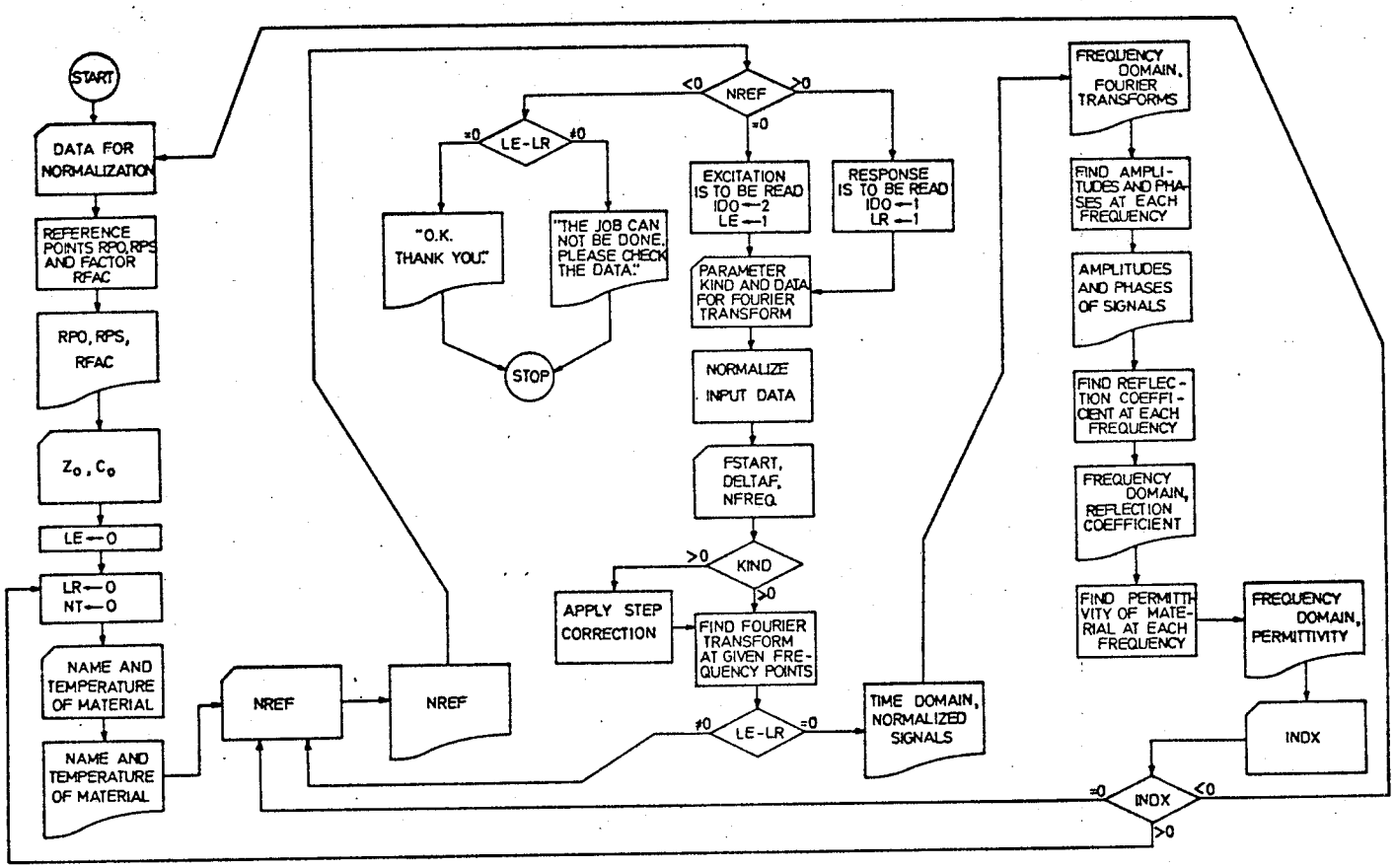

Fig. 6.2. The simplified flowchart of the system software.

6. The input data of the signal is normalized in the time domain and the Fourier Transform is evaluated using the formula: $$F_{Ts}(\omega)=\Delta T\sum_{n=0}^{N-1} f(n\Delta T)\, e^{-jn\omega\Delta T}$$

   If the parameter KIND is less than zero, the step correction /16/ is applied to decrease the truncation error.

7. The program control is transfered to step 3 and steps 3, 4, 5 and 6 are repeated for the next data set.

8. Both excitation and response signals have already been stored in the computer memory, and thus the normalized time domain signals and their Fourier Transforms /real and imaginary parts/ are printed out.

9. The amplitudes and phases of both signals are evaluated and printed out.

10. The amplitude and phase, Eq. /4.5/, of the input reflection coefficient of the sample holder are found and printed out.

11. The dielectric constant and loss factor of the test material are calculated, Eqs. /4.2. and 4.3./, and printed out.

12. The input control parameter INDX is read and the program control is transfered depending on the value of INDX:

/a/ if INDX = 0, the control is transfered to step 3 to check if there is more data for the same material,

/b/ if INDX > 0, the control is transfered to step 2 to perform computations for a different sample,

/c/ if INDX < 0, the control is transfered to the step 1 to start a new normalization.

The software was tested with different data sets and was found convenient and flexible in processing the experimental data.

CHAPTER 7

EXPERIMENTAL VERIFICATION

The performance of the system was verified experimentally by measurements of the dielectric properties of some normal alcohols. The sample holder having a capacitance of 0.2923 pF was used in the reported experiments. The computations were done by an IBM-360 computer employing the system software discussed in section 6.2. The step correction was applied /parameter KIND = - 1/ to all transformations into the frequency domain. The compilation time of the program was approximately 0.8 second, while the typical execution time was 10 seconds for approximately 400 data points for each substance.

The experimental results in Fig. 7.1 through Fig. 7.6 are generally in good agreement with the Cole-Cole semicircle with a single relaxation time. The experimental semicircles are slightly shifted to the left as compared with the results given by /12/ and /14/. This is probably due to the uncertainties in the air line of the sample holder and possible errors in the capaciatance of the empty sample holder and the characteristic impedance of the line.

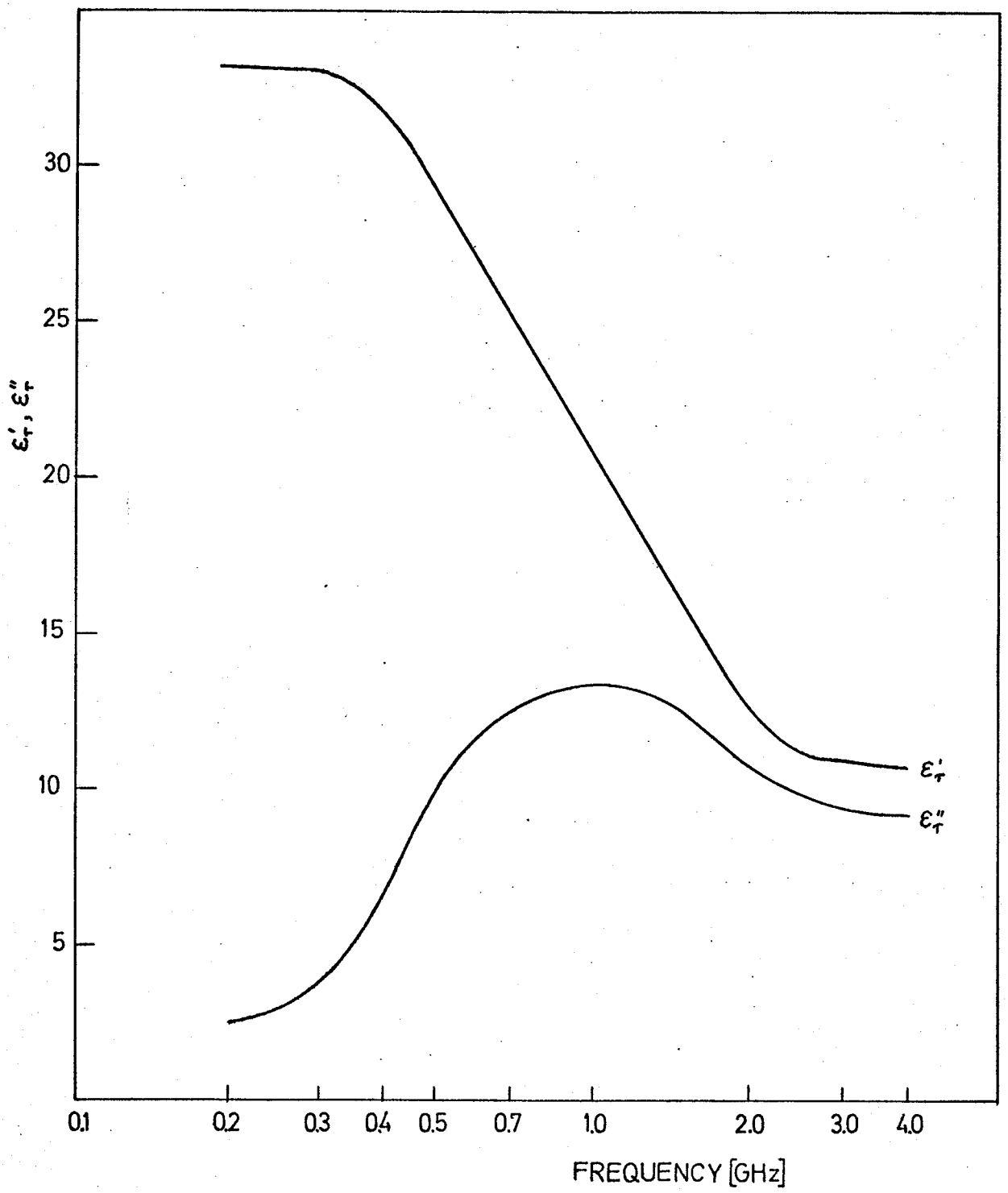

Fig.7.1. Experimental results for methanol at 24.5° C.

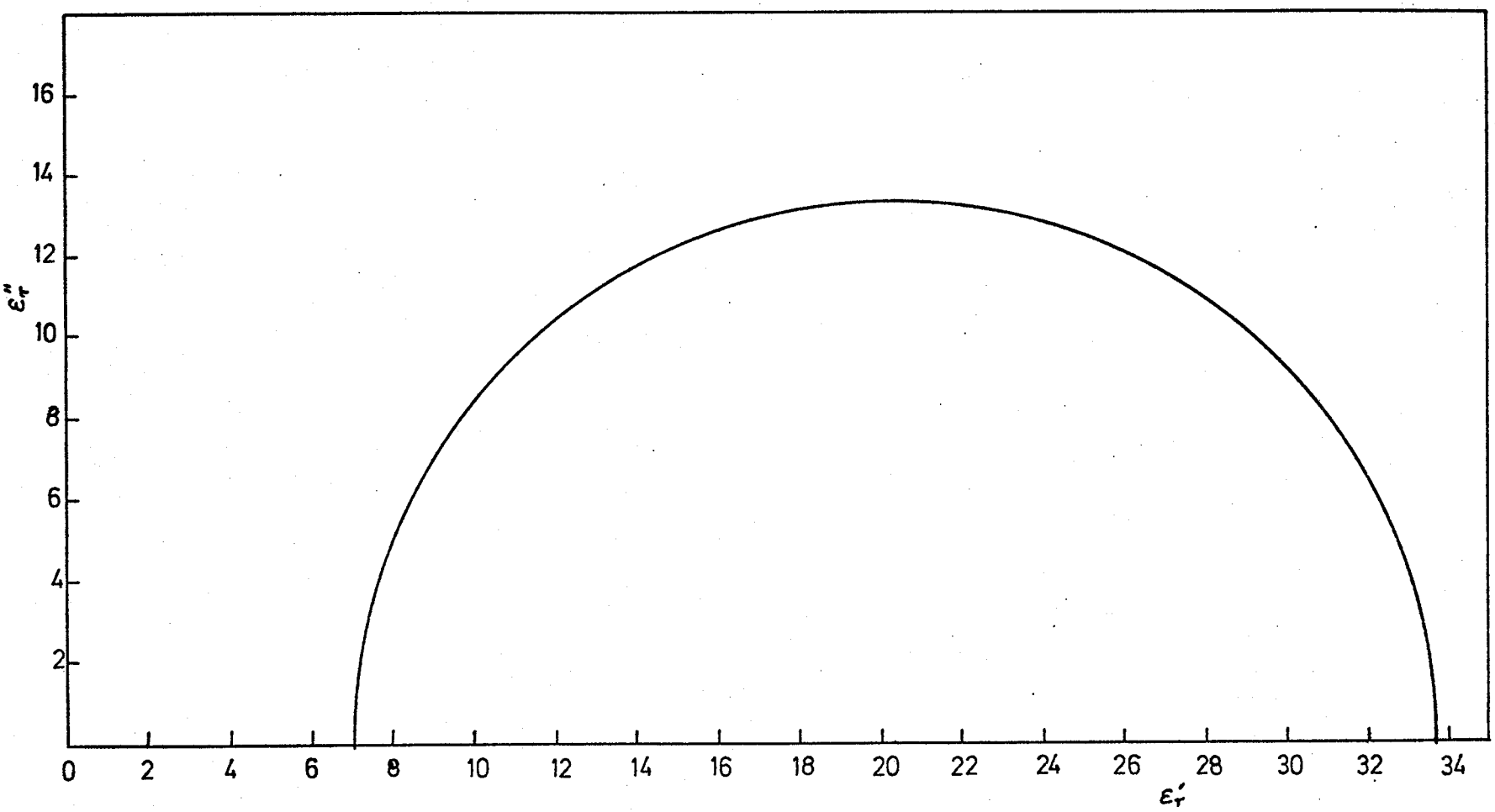

Fig.7.2. Experimental results for methanol at 24.5 °C presented in the Cole-Cole form.

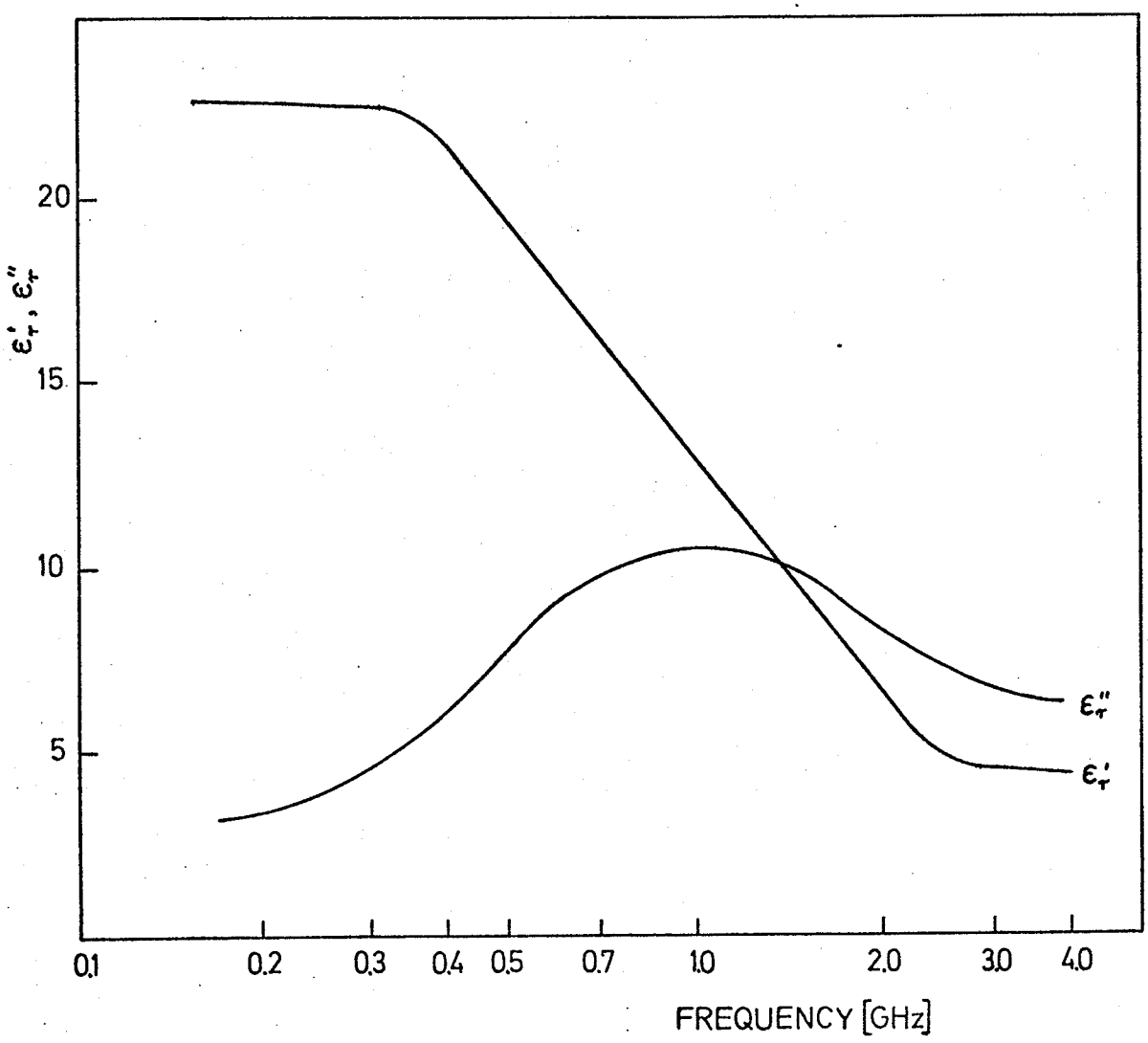

Fig.7.3. Experimental results for ethanol at 24.5 °C.

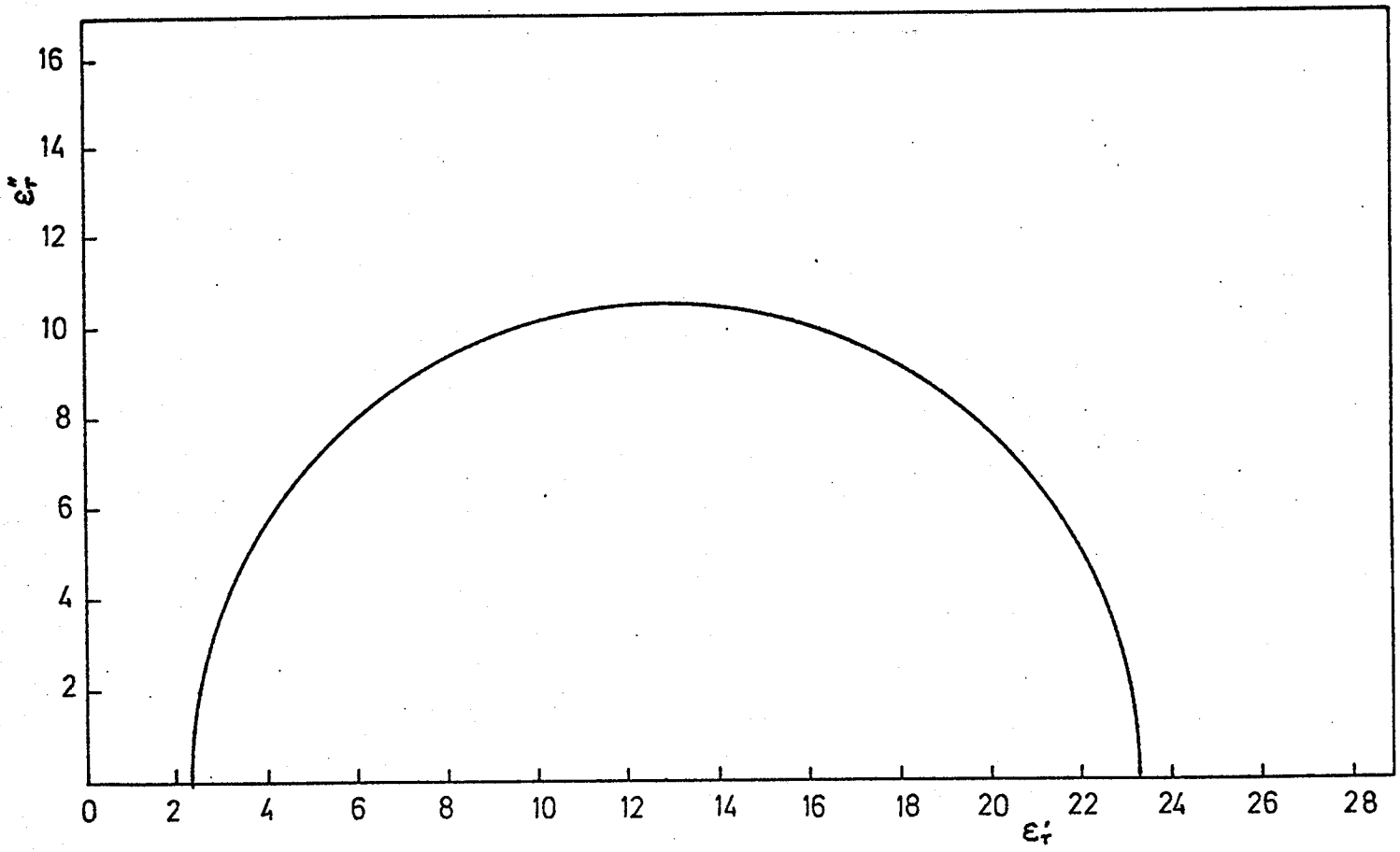

Fig.7.4. Experimental results for ethanol at 24.5 °C presented in the Cole-Cole form.

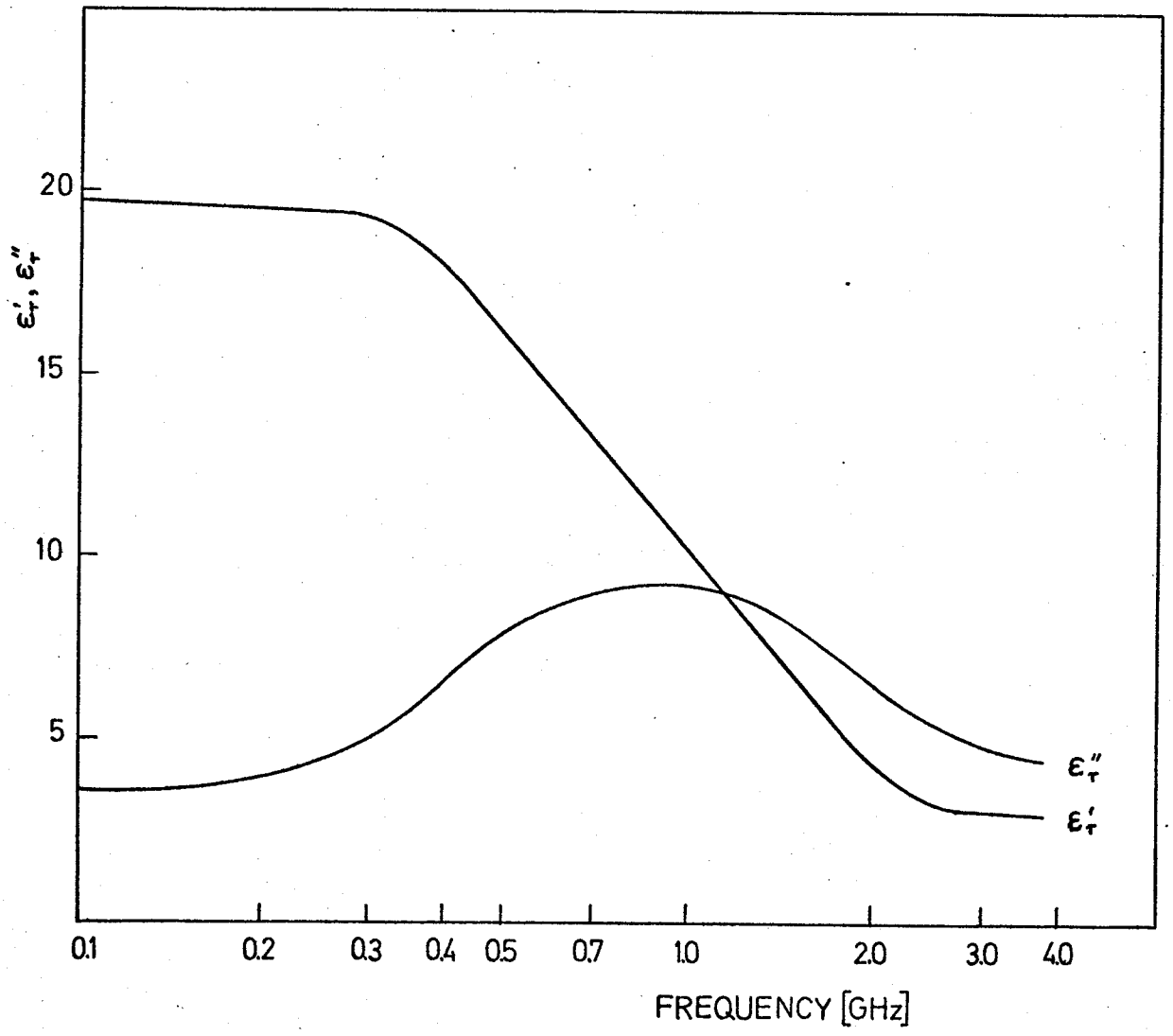

Fig.7.5. Experimental results for n-propanol at 25 °C.

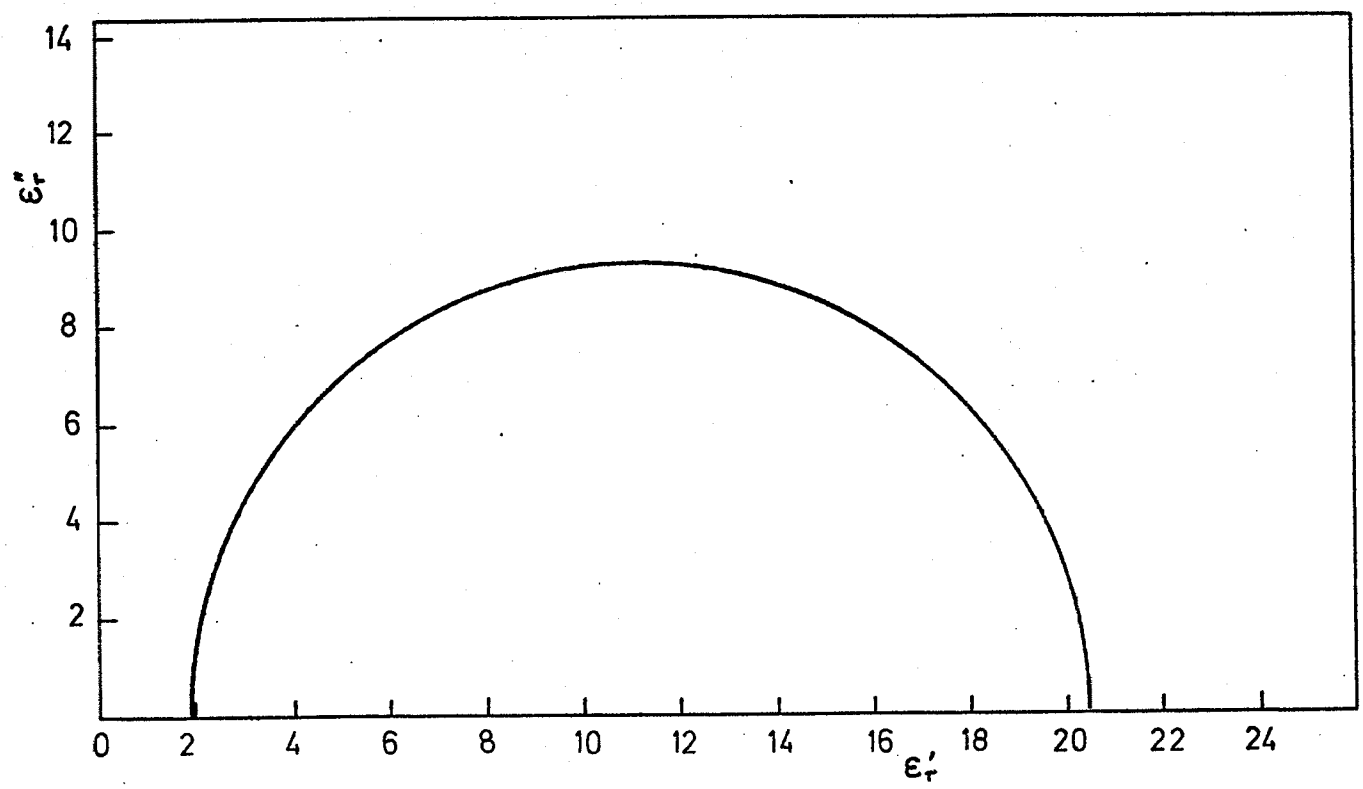

Fig.7.6. Experimental results for n-propanol at 25 ^{o}C presented in the Cole-Cole form.

CHAPTER 8

SUMMARY AND CONCLUSIONS

An experimental system for fast permittivity measurements in the time domain has been investigated.

The need for fast measurements in investigations of the dielectric properties of biological substances has been discussed. Definitions of basic quantities describing dielectrics and explanations of different mechanisms of the dielectric polarization have been presented.

Both the frequency domain and time domain methods and techniques for determination of the dielectric properties have been reviewed and compared. The time domain measurement technique based on the lumped capacitance method has been found most suitable for fast permittivity measurements over a wide frequency range.

The inherent advantages of the measurement method have been discussed and a typical time domain experimental setup described. On this basis, the requirements for an experimental system for fast permittivity measurements have been formulated. The system has been designed and developed to include a sample holder, an automatic analog to digital converter and an interface and control unit.

The interface and control unit has been built to interface all the esential parts of the experimental system and

to provide automatic control of the whole system. The possibilities of using an external clock and utilizing the A/D converter with an equipment other than the TDR system are provided. The unique features are the start and stop points of the analog to digital conversion which can be adjusted according to current needs.

Software for performing all computations necessary for finding the permittivity of a test material has been developed. The software provides normalization of the experimental data, transformation into the frequency domain, evaluation of the amplitude and phase of the input reflection coefficient of the sample holder and calculations of the dielectric constant and loss factor of a test material.

The experimental system /including hardware and software/ has been thoroughly tested and found satisfactory, simple, and flexible in both measurement procedure and data processing. The system is particulary suitable for fast measurements of the dielectric properties of biological substances.

Higher speed of measurements can be achieved by eliminating the human participation in preparation of the data for the computer. One of the following solutions is suggested for further increasing the speed of measurements:

1. A Hewlett-Packard Model 3489A Data Punch can be used as an output device of the experimental system. In this case the output data would be punched on a paper

tape. The tape can be read by an optical reader of a digital computer. This arrangement would cost approximately $ 3,500.

2. A Hewlett-Packard Model 2570 A Coupler /Controler with an HP 12797 A BCD Input Card can be connected directly to the output of the analog to digital converter. In this case the system output data would be fed into a computer through an acoustic coupler and a telephone line. This arrangement would cost approximately $ 5,000.
3. The analog to digital converter can be connected to a minicomputer through a code converter /BCD to ASCII/. In this case the experimental data would be fed directly to the minicomputer which would perform all the computations necessary for finding the permittivity of a test material. In addition, the minicomputer can control all the measurements working in a feedback loop with the experimental system, thus setting up an independent self controled automatic system. Total cost of this arrangement at present is estimated to be $25,000 to $50,000 depending on the minicomputer used.

REFERENCES

/1/ Nelson, S.O., "Electrical Properties of Agricultural Products. A Review", for presentation at the 1971 Winter Meeting American Society of Agricultural Engineers, Chicago, Illinois, December 1971.

/2/ Franceschetti, G., "A Complete Analysis of the Reflection and Transmission Methods for Measuring the Complex Permeability and Permittivity of Materials at Microwaves", Alta Freq., Vol. 36, p. 757, 1967.

/3/ Von Hippel, A.R., Dielectric Materials and Applications, J. Wiley, New York 1954.

/4/ Böttcher, C.J.F., Theory of Electric Polarization, Elsevier Publishing Company, 1952.

/5/ Hill, N.E., Vaughan, W.E., Price, A.H. and Davies M., Dielectric Properties and Molecular Behaviour, Van Nostrand Reinhold Company, London 1969.

/6/ Westphal, W.B., Dielectric Materials and Applications, A.R. von Hippel, Ed., J. Wiley, New York 1954.

/7/ Bussey, H.E., "Measurement of RF Properties of Materials - A Survey", Proc. IEEE, Vol. 55, pp. 1046-1053, 1967.

/8/ Rzepecka, M.A., Stuchly, S.S. and Hamid, M.A.K., "Modified Infinite Sample Method for Routine Permittivity Measurements at Microwave Frequencies", IEEE Trans. Instrum. Meas., Vol. IM-22, No. 1, pp. 41-46, 1973.

/9/ Wenger, N.C. and Smetana, J., "Hydrogen Density Measure-

ments Using an Open-Ended Microwave Cavity", IEEE Trans.Instrum. Meas., Vol. IM-21, pp. 105-114, 1972.

/10/ Stuchly, S.S., Rzepecka, M.A. and Hamid, M.A.K., "A Microwave Open-Ended Cavity as a Void Fraction Monitor for Organic Coolants", IEEE Trans., Vol. IECI-21, No. 2, pp. 78-80, 1974.

/11/ van Gemert, M.J.C., "High-Frequency Time-Domain Methods in Dielectric Spectroscopy", Philips Res. Repts 28, 530-572, 1973.

/12/ van Gemert, M.J.C., "Time-Domain Reflectometry as a Method for the Examination of Dielectric Relaxation Phenomena in Polar Liquids", Ph.D. dissertation, Leiden, 1972.

/13/ Iskander, M.F. and Stuchly, S.S., "A Time-Domain Technique for Measurement of the Dielectric Properties of Biological Substances", IEEE Trans. Instrum. Meas., Vol. IM-21, No. 4, pp. 425-429, 1972.

/14/ Stuchly, S.S., Rzepecka, M.A. and Iskander, M.F., "Permittivity Measurements at Microwave Frequencies Using Lumped Elements", IEEE Trans. Instrum. Meas., Vol. IM-23, No.1, pp. 56-62, 1974.

/15/ Rzepecka, M.A. and Stuchly, S.S., "A Lumped Capacitance Method for the Measurement of the Permittivity and Conductivity in the Frequency and Time Domain - A Further Analysis", to be published.

/16/ Ross, G.F., Nicolson, A.M., Smith, R., Susman, L., and Hanley, G., "Transient Behaviour of Microwave Networks", Sperry Rand Research Center, Report No. SRRC-CR-68-2, 1968.

APPENDIX A

SCHEMATIC DIAGRAMS

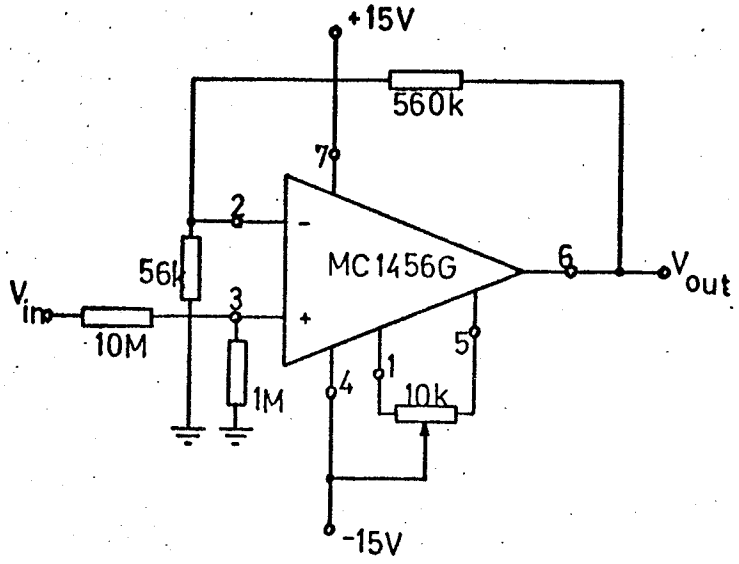

Fig.A.1. Schematic diagram of the Buffer Amplifier.

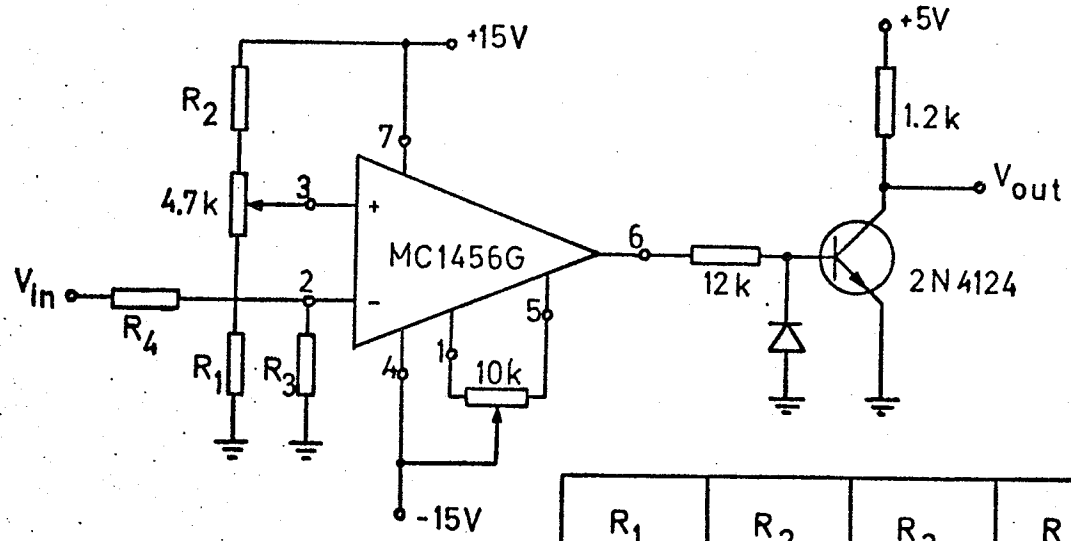

	R_1	R_2	R_3	R_4
INITIATE COMPARATOR	3.3k	10k	220k	1M
SCAN SWITCH COMPARATOR	4.7k	10k	2M	20M

Fig.A.2. Schematic diagram of the Scan Switch and Initiate Comparators and the Limiter/Inverter.

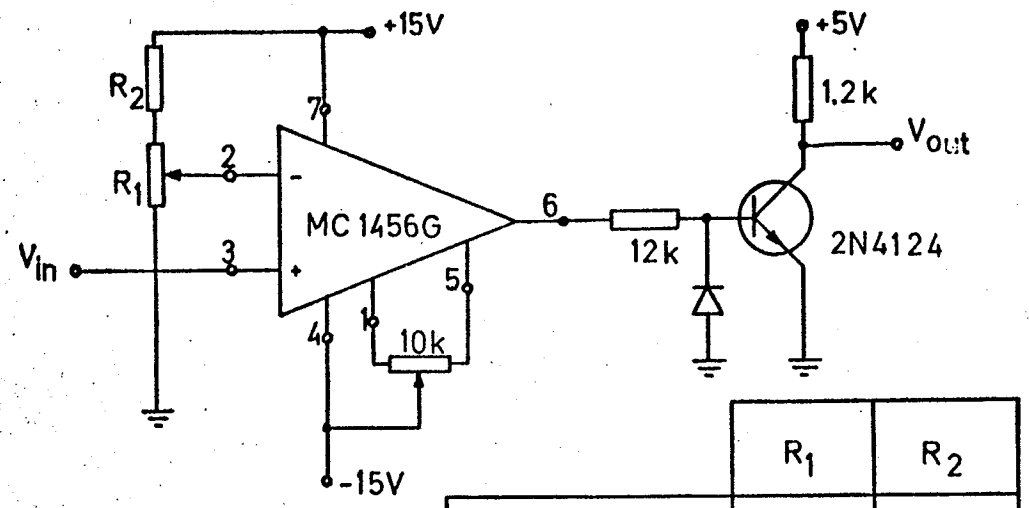

	R_1	R_2
PROGRAM EXECUTE COMPARATOR	470	27 k
STOP MARKER COMPARATOR	20 k	6.8k

Fig.A.3. Schematic diagram of the Program Execute and Stop Marker Comparators and the Limiter/Inverter.

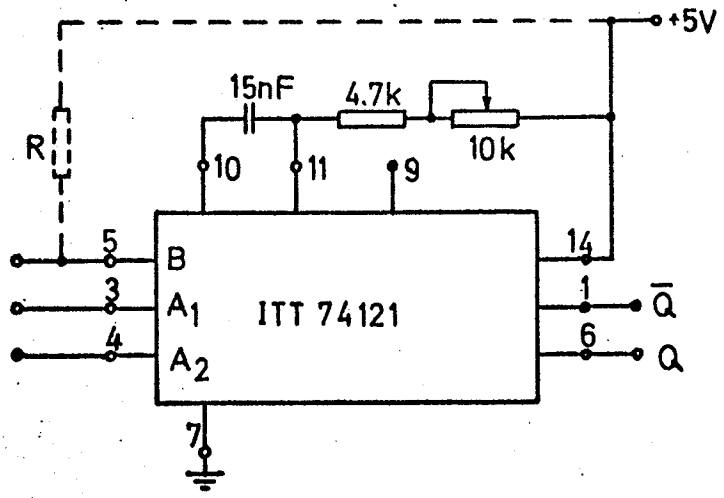

Negative edge trigger, input - pin 3 or 4, pin 5 connected to +5V through R = 4.7k Ω.

Positive edge trigger, input - pin 5, pin 3 and 4 grounded.

Fig.A.4. Schematic diagram of Monostable Multivibrators.

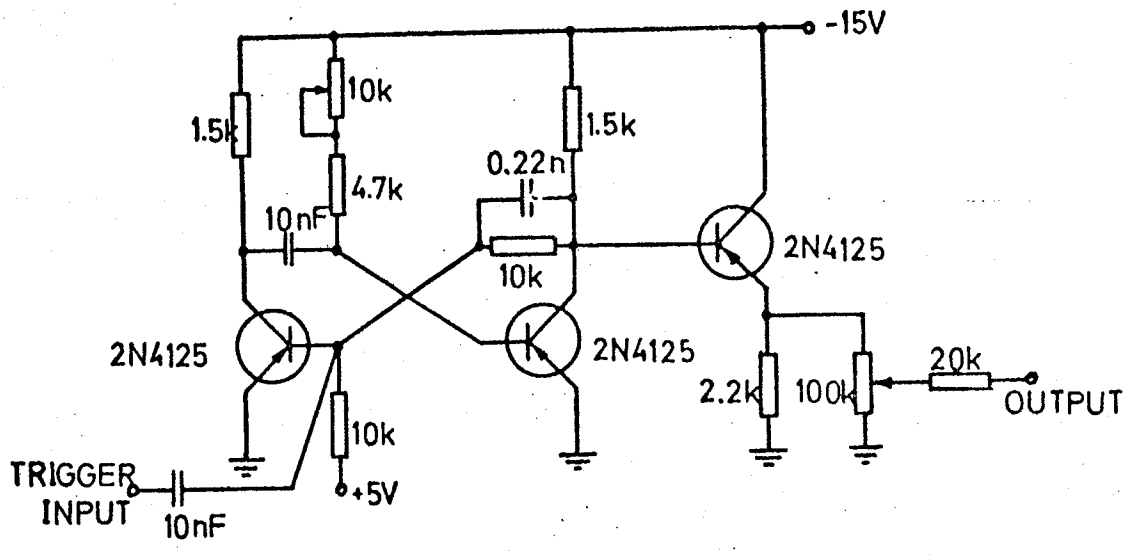

Fig.A.5. Schematic diagram of the Stop Marker Monostable Multivibrator.

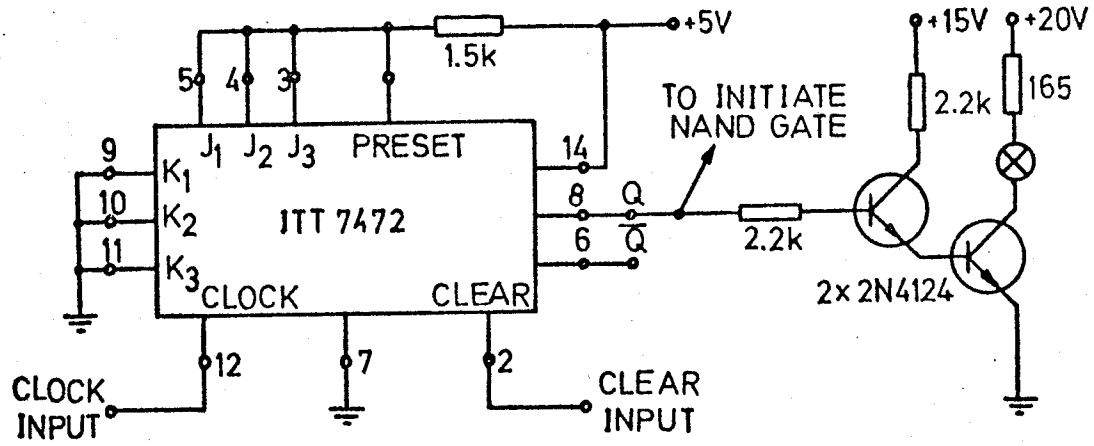

Fig.A.6. Schematic diagram of the Program Acknowledgement Flip-Flop and the Light Indicator.

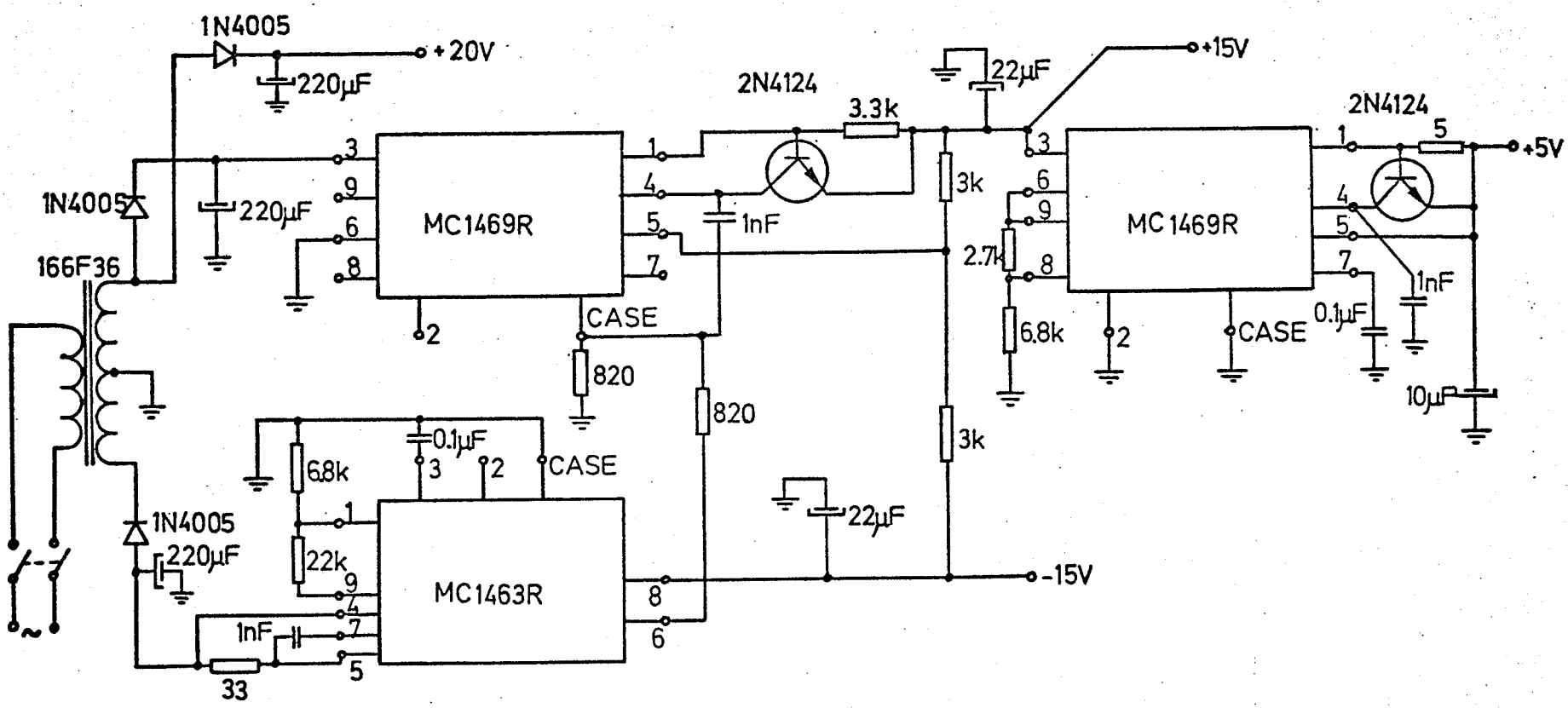

Fig.A.7. Schematic diagram of the power supply.

APPENDIX B

CABLE CONNECTIONS

Table B.1. Cable connection between the TDR plug-in and the interface and control unit.

Point in the TDR circuit	TDR plug-in rear connector	Colour of the wire	Cable connector
927	PI - 5	red	A
903	PI - 4	black	H
TP5	PI - 9	green	P
TP3	PI - 25	white	W
chassis		shield	c

Table B.2. Input cable to the scanner /channel 1/

Scanner rear input connector	Description	Colour of the wire	BNC connector
c	"guard"	white and shield	outer conductor
a	"1 LO "	green	
Z	"1 HI "	black and red	inner pin

Table B.3. Remote control signals cable

Remote control cable connector /male/	Colour of the wire	Control Signals
A	white	"Home"
E	green	"External Trigger"
d	red	"Initiate"
a	black	"Program Execute"
S	shield	Ground
K	white	"Step Program"
T	red	"Continuous Scan Program"
z	green	"Program Acknowledge"
c	black	"Random Program"
N - S	bare	"10V Range"
W - S	bare	"1 Program"

APPENDIX C

COMPUTER PROGRAM

The computer program discussed in details in section 6.2 is written in WATFIV. The program performs all the computations necessary for finding the dielectric constant and the loss factor of a test material.

```
      $JOB  WATFIV  M.T. FABER
      C PERMITTIVITY MEASUREMENTS IN TIME DOMAIN
    1       DIMENSION A(1000),B(500),AN(2,1000),BF(500)
    2       DIMENSION C(2,500),D(2,500),CT(2,500),DT(2,500),DELTAT(2)
    3       DIMENSION NAME(20)
      C START NORMALIZATION
      C FIND THE REFERENCE POINT RPO(GAMMA=0)
    4    97 READ,NPO
    5       READ,((C(1,I),I=1,NPO)
    6       RPO=0.0
    7       DO 6 I=1,NPO
    8     6 RPO=RPO+C(1,I)
    9       RPO=RPO/NPO
      C FIND THE REFERENCE POINT RPS(GAMMA=1)
   10       READ,NPS
   11       READ,((C(2,I),I=1,NPS)
   12       RPS=0.0
   13       DO 7 I=1,NPS
   14     7 RPS=RPS+C(2,I)
   15       RPS=RPS/NPS
      C FIND NORMALIZATION FACTOR RFAC
   16       RFAC=RPS-RPO
   17       PRINT120,RPO,RPS,RFAC
   18       DO 102 I=1,2
   19       DO 103 K=1,1000
   20   103 AN(I,K)=1.0
   21   102 CONTINUE
   22       READ,ZO,CO
   23       LE=0
   24    99 LR=0
   25       NT=1
   26       READ105,NAME
   27       PRINT110,NAME
   28     2 READ,NREF
   29       PRINT125,NREF
   30       IF(NREF) 3,8,9
      C 3-NO MORE DATA SETS
      C 8-NORMALIZE THE EXCITATION
      C 9-NORMALIZE THE RESPONSE
   31     8 IDO=2
   32       LE=1
   33       GO TO 11
   34     9 IDO=1
   35       LR=1
   36    11 PI=3.141592654
   37       P2=PI+PI
   38       PO2=PI/2.
   39       FAC=180./PI
   40       READ,N1,N,T,KIND
   41       IF(N.GT.NT) NT=N
   42       READ,RPT
   43       READ,(A(I),I=1,N)
   44       DO 12 I=1,N
   45       PRINT130,A(I)
   46    12 AN(IDO,I)=(A(I)-RPT)/RFAC
      C END OF NORMALIZATION
      C FIND THE FOURIER TRANSFORM
   47       DELTAT(IDO)=T/N1
   48       READ,FSTART,DELTAF,NFREQ
   49       IMAX=NFREQ+1
   50       Z=P2*DELTAT(IDO)
   51       BF(1)=FSTART
   52       DO 29 I=2,IMAX
   53    29 BF(I)=BF(I-1)+DELTAF
```

```
      DO 13 I=1,IMAX
      WH=BF(I)*Z
      R=0.0
      S=0.0
      T=0.0
      DO 14 L=1,N
      R=R+AN(IDO,L)*COS(T)
      S=S-AN(IDO,L)*SIN(T)
      T=T+WH
   14 CONTINUE
      IF(KIND) 38,39,39
C 38-APPLY THE STEP CORRECTION
C 39-DO NOT APPLY THE STEP CORRECTION
   38 IF(WH-1.E-6) 39,40,40
   40 X=AN(IDO,N)/(2.*SIN(WH/2.))
      Y=WH*(N-.5)+P02
      R=R+X*COS(Y)
      S=S-X*SIN(Y)
   39 C(IDO,I)=R
C R-REAL PART/DELTAT
      D(IDO,I)=S
C S-IMAGINARY PART/DELTAT
   13 CONTINUE
      LL=LE-LR
      IF(LL.NE.0) GO TO 2
C READ THE NEXT DATA SET
      PRINT135
      PRINT140
      TE=0.0
      TR=0.0
      DO 4 I=1,NT
      PRINT145,TE,AN(2,I),TR,AN(1,I)
      TE=TE+DELTAT(2)
      TR=TR+DELTAT(1)
    4 CONTINUE
C THE EXCITATION AND RESPONSE HAVE BEEN TRANSFORMED IN =REQUENCY DOMAIN
      PRINT150
      PRINT155
      PRINT160
      DO 5 I=1,IMAX
      PRE=DELTAT(2)*C(2,I)
      PIE=DELTAT(2)*D(2,I)
      PRR=DELTAT(1)*C(1,I)
      PIR=DELTAT(1)*D(1,I)
      PRINT165,BF(I),PRE,PIE,PRR,PIR
    5 CONTINUE
C FIND THE AMPLITUDE AND PHASE
      DO 1 IDO=1,2
      IO=-1
      I1=-1
      B0=-.002
      B1=-.001
      IND=-1
      DO 10 I=1,IMAX
      R=C(IDO,I)
      S=D(IDO,I)
      CT(IDO,I)=DELTAT(IDO)*SQRT(R*R+S*S)
C CT-AMPLITUDE
      THETA=ATAN(S/R)
      IF(R) 16,15,15
   15 I2=1
      GO TO 17
   16 I2=-1
   17 IF(S) 19,18,18
```

```
110      18 I2=I2+2
111         GO TO 81
112      19 I2=I2-2
113      81 IF(I2-3) 21,20,21
114      21 IF(I2-1) 22,23,22
115      22 IF(I2+3) 24,23,24
116      24 THETA=THETA+6.283185
117         GO TO 20
118      23 THETA=THETA+3.14159265
119      20 I3=4*I1-I2
120         IF(I3-13) 41,55,41
121      41 IF(I3+15) 42,70,42
122      42 IF(I3+7) 43,70,43
123      43 IF(I3+5) 45,70,45
124      45 IF(I3-1) 46,54,46
125      46 IF(I3+1) 49,54,49
126      49 IF(I3+13) 80,54,80
127      55 IF(I0-I1) 71,51,71
128      51 IF(B0-B1) 80,71,80
129      54 IF(I0-I1) 80,52,80
130      52 IF(B1-B0) 80,70,80
131      70 IND=IND+1
132         GO TO 80
133      71 IND=IND-1
134      80 THETA=THETA+6.283185*IND
135         DT(IDO,I)=THETA
      C DT-PHASE
136         I0=I1
137         I1=I2
138         B0=B1
139         B1=THETA
140      10 CONTINUE
141       1 CONTINUE
142         PRINT150
143         PRINT155
144         PRINT170
145         DO 27 I=1,IMAX
146         PHE=FAC*DT(2,I)
147         PHR=FAC*DT(1,I)
148         PRINT115,BF(I),CT(2,I),PHE,CT(1,I),PHR
149      27 CONTINUE
150         PRINT150
151         PRINT175
152         PRINT180
      C FIND THE AMPLITUDE AND PHASE OF REFLECTION COEFFICIENT
153         DO 62 I=1,IMAX
154         B(I)=CT(1,I)/CT(2,I)
155         A(I)=DT(1,I)-DT(2,I)
156         PH=FAC*A(I)
157         PRINT185,BF(I),B(I),PH
158      62 CONTINUE
159         PRINT190
160         PRINT195
      C FIND PERMITTIVITY OF THE TESTED MATERIAL
161         DO 65 I=1,IMAX
162         Z=BF(I)
163         X=B(I)
164         Y=A(I)
165         AP=COS(Y)
166         R=SIN(Y)
167         XX=X*X
168         YY=2.*X*AP
169         H=P2*Z*Z0*C0
170         HH=XX+YY+1.0
```

```
171          E1=-(2.*X*R)/(H*HH)
172          E11=(1.-XX)/(H*HH)
173          PRINT200,Z,E1,E11
174       65 CONTINUE
175          READ,INDX
176          IF(INDX) 97,2,99
         C 97-START A NEW NORMALIZATION
         C  2-CHECK IF THERE IS AN OTHER DATA SET FOR THE SAME SAMPLE
         C 99-PERFORM COMPUTATIONS FOR THE RESPONSE OF A NEW SAMPLE
177         3 IF(LE-LR.NE.0) GO TO 68
178          PRINT205
         C THE JOB HAS BEEN DONE
179          GO TO 69
180       68 PRINT210
         C WRONG DATA, THE JOB CAN NOT BE DONE
181       69 STOP
182      105 FORMAT(20A4)
183      110 FORMAT('-',20A4)
184      115 FORMAT(' ',E16.5,F15.5,F10.2,7X,E12.5,F10.2)
185      120 FORMAT('1',5X,'NORMALIZATION: RPO=',F7.3,5X,'RPS=',F7.3,5X,'RFAC='
           C,F7.3)
186      125 FORMAT('0',I17)
187      130 FORMAT(' ',10X,F7.3)
188      135 FORMAT('-',28X,'TIME DOMAIN')
189      140 FORMAT('0',10X,'TIME',6X,'EXCITATION',9X,'TIME',7X,'RESPONSE')
190      145 FORMAT(' ',4X,E12.5,F12.4,5X,E12.5,F12.4)
191      150 FORMAT('-',25X,'FREQUENCY DOMAIN')
192      155 FORMAT('0',10X,'FREQ.',12X,'EXCITATION',17X,'RESPONSE')
193      160 FORMAT(' ',18X,'REAL AND IMAGINARY PARTS',5X,'REAL AND IMAGINARY P
           CARTS')
194      165 FORMAT(' ',E16.4,2E13.4,3X,2E13.4)
195      170 FORMAT(' ',22X,'AMPLITUDE AND PHASE',9X,'AMPLITUDE AND PHASE')
196      175 FORMAT('0',22X,'REFLECTION COEFFICIENT')
197      180 FORMAT(' ',11X,'FREQ.',12X,'AMPLITUDE',9X,'PHASE')
198      185 FORMAT(' ',E17.5,F19.5,F16.5)
199      190 FORMAT('-',30X,'PERMITTIVITY')
200      195 FORMAT('0',11X,'FREQ.',15X,'E1',15X,'E11')
201      200 FORMAT(' ',E17.5,2F18.5)
202      205 FORMAT('-',20X,'O.K. THANK YOU')
203      210 FORMAT('-',10X,'SORRY,THE JOB CAN NOT BE DONE. PLEASE CHECK THE DA
           CTA')
204          END

         $ENTRY
```